

**Carderock Division, Naval Surface Warfare Center**  
**West Bethesda, Maryland 20817-5700**

---

NSWCCD-50-TR-2006/020 April 2006  
Hydromechanics Department Report

**MODEL 5514 CAPSIZE EXPERIMENTS  
REPRESENTING THE PRE-CONTRACT DDG51  
HULL FORM AT END OF SERVICE LIFE  
CONDITIONS**

By  
David Dantagnan Hayden  
Richard C. Bishop  
Joel T. Park  
Stephen M. Laverty



---

Approved for public release; distribution is unlimited.

---

# REPORT DOCUMENTATION PAGE

Form Approved  
OMB No. 0704-0188

Public reporting burden for this collection of information is estimated to average 1 hour per response, including the time for reviewing instructions, searching existing data sources, gathering and maintaining the data needed, and completing and reviewing this collection of information. Send comments regarding this burden estimate or any other aspect of this collection of information, including suggestions for reducing this burden to Department of Defense, Washington Headquarters Services, Directorate for Information Operations and Reports (0704-0188), 1215 Jefferson Davis Highway, Suite 1204, Arlington, VA 22202-4302. Respondents should be aware that notwithstanding any other provision of law, no person shall be subject to any penalty for failing to comply with a collection of information if it does not display a currently valid OMB control number. **PLEASE DO NOT RETURN YOUR FORM TO THE ABOVE ADDRESS.**

<b>1. REPORT DATE (MM/DD/YYYY)</b> 4/14/2006		<b>2. REPORT TYPE</b> Final		<b>3. DATES COVERED (From - To)</b> 09/01/2004 - 09/30/2005	
<b>4. TITLE AND SUBTITLE</b> MODEL 5514 CAPSIZE EXPERIMENTS REPRESENTING THE PRE-CONTRACT DDG51 HULL FORM AT END OF SERVICE LIFE CONDITIONS				<b>5a. CONTRACT NUMBER</b>	
				<b>5b. GRANT NUMBER</b>	
				<b>5c. PROGRAM ELEMENT NUMBER</b> 64300N	
				<b>5d. PROJECT NUMBER</b>	
<b>6. AUTHOR(S)</b> David Dantagnan Hayden Richard C. Bishop Joel T. Park Stephen M. Laverty				<b>5e. TASK NUMBER</b>	
				<b>5f. WORK UNIT NUMBER</b> 05-1-5500-616	
				<b>8. PERFORMING ORGANIZATION REPORT NUMBER</b>  NSWCCD-50-TR-2006/020	
<b>7. PERFORMING ORGANIZATION NAME(S) AND ADDRESS(ES) AND ADDRESS(ES)</b>  Naval Surface Warfare Center Carderock Division Seakeeping Division-5500 9500 Macarthur Boulevard West Bethesda, MD 20817-5700				<b>9. SPONSORING / MONITORING AGENCY NAME(S) AND ADDRESS(ES)</b>  NAVSEA PMS500 1333 Isaac Hull Ave. SE Washington, D.C. 20376	
<b>12. DISTRIBUTION / AVAILABILITY STATEMENT</b> Approved for public release; distribution is unlimited.				<b>10. SPONSOR/MONITOR'S ACRONYM(S)</b> NAVSEA PMS500	
				<b>11. SPONSOR/MONITOR'S REPORT NUMBER(S)</b>	
<b>13. SUPPLEMENTARY NOTES</b>					
<b>14. ABSTRACT</b> <p>The DDG51 pre-contract hull form as represented by Model 5514 was evaluated for capsizes events at End of Service Life Load Limit for the Righting Arm Limiting and Intact 100 Knot Wind Limiting KG Conditions. The results are compared to FREDYN 9.3 predictions, and results from previous Model 5514 capsizes experiments. Results are also presented for a limited number of calm water maneuvering and irregular wave tests. The results are to be used as benchmarks for comparison with capsizes results observed for future hull forms as compared to conventional hull forms.</p>					
<b>15. SUBJECT TERMS</b> DDG51, Capsizes Experiments, Seakeeping, Model Experiments					
<b>16. SECURITY CLASSIFICATION OF:</b>			<b>17. LIMITATION OF ABSTRACT</b>  SAR	<b>18. NUMBER OF PAGES</b>  82	<b>19a. NAME OF RESPONSIBLE PERSON</b> Dan Hayden
<b>a. REPORT</b> UNCLASSIFIED	<b>b. ABSTRACT</b> UNCLASSIFIED	<b>c. THIS PAGE</b> UNCLASSIFIED			<b>19b. TELEPHONE NUMBER (include area code)</b> (301) 227-5932

Standard Form 298 (Rev. 8-98)  
Prescribed by ANSI Std. Z39.18



## CONTENTS

ABSTRACT .....	1
ADMINISTRATIVE INFORMATION.....	1
ACKNOWLEDGEMENTS .....	1
INTRODUCTION.....	2
MODEL DESCRIPTION.....	2
Hull Configuration.....	3
Model Propulsion and Control .....	4
Instrumentation, Information, and Intelligence Control .....	5
FACILITIES .....	7
Test Basin.....	7
Wave Generation and Measurement .....	8
Tethered Carriage Operation .....	8
Free Running Model.....	8
Tracking System .....	9
EXPERIMENTAL PROCEDURE.....	9
Wavemaker Settings.....	9
Roll Decay .....	10
Speed Calibration .....	10
Maneuvering Runs – FREDYN Correlation .....	10
Regular Wave Capsize.....	12
Irregular Wave Seakeeping .....	13
UNCERTAINTY ANALYSIS.....	13
Acceleration .....	14
Pitch and Roll Angle .....	15
Model Velocity and Propeller Shaft Speed.....	15
Heading .....	17
Rudder Angle .....	17
Rudder Angular Rate .....	17
Wave Height Gage .....	18
RESULTS .....	18
Waves Settings.....	18
Roll Decay .....	18
Maneuvering.....	19
Dynamic Stability – Capsize Evaluation.....	20
Seakeeping .....	21
SUMMARY AND CONCLUSIONS .....	22
REFERENCES.....	69

## FIGURES

1. View of Model 5514 During Capsize Testing In MASK Basin. ....	23
2. Model 5514 as Configured for Testing – Bow and Stern Top Views. ....	25
3. Model Arrangements at Mid-Ship Including GM Pole, and Battery Access Hatch. ....	27
4. GZ Curve for Pre-Contract DDG51, Model 5514. ....	27
5. Propellers and Rudders for Model 5514. ....	29
6. On Board Computer (OBC) of Model 5514. ....	29
7. Sketch of Maneuvering and Seakeeping (MASK) Basin. ....	31
8. Relative Position of Bridge Sonics When Bridge Is At 30 Degrees. ....	32
9. Residuals for calibration of acceleration at CG for model 5514. ....	33
10. Residuals for calibration of roll angle for model 5514. ....	34
11. Residuals for calibration of propeller shaft rotational speed. ....	34
12. Residuals for calibration of model velocity for model 5514 from propeller shaft speed. ....	35
13. Comparison of model velocity from tracker to stopwatch data. ....	36
14. Comparison of tracker to model heading for model 5514. ....	36
15. Residuals for calibration of rudder angle for model 5514. ....	37
16. Residuals for calibration of Senix wave height gage #1. ....	37
17. Roll Periods for End of Service Life, Intact 100kt Wind Limited KG. ....	38
18. Roll Periods for End of Service Life, Righting Arm Limited KG. ....	38
19. Roll Decay Coefficients for End of Service Life, Intact 100kt Wind Limited KG, $F_n=0.0$ . ....	39
20. Roll Decay Coefficients for End of Service Life, Intact 100kt Wind Limited KG, $F_n=0.1$ . ....	39
21. Roll Decay Coefficients for End of Service Life, Intact 100kt Wind Limited KG, $F_n=0.2$ . ....	40
22. Roll Decay Coefficients for End of Service Life, Intact 100kt Wind Limited KG, $F_n=0.3$ . ....	40
23. Roll Decay Coefficients for End of Service Life, Intact 100kt Wind Limited KG, $F_n=0.4$ . ....	41
24. Roll Decay Coefficients for End of Service Life, Righting Arm Limited KG, $F_n=0.0$ . ....	41
25. Roll Decay Coefficients for End of Service Life, Righting Arm Limited KG, $F_n=0.1$ . ....	42
26. Roll Decay Coefficients for End of Service Life, Righting Arm Limited KG, $F_n=0.2$ . ....	42
27. Roll Decay Coefficients for End of Service Life, Righting Arm Limited KG, $F_n=0.3$ . ....	43
28. Roll Decay Coefficients for End of Service Life, Righting Arm Limited KG, $F_n=0.4$ . ....	43
29. Plot and Curve Fit of Tactical Diameter Versus Rudder Angle for all Speeds. ....	44
30. Example Zig-Zag Maneuver – Run 172. ....	44
31. Time Histories Reviewed to Assure Quality of Capsize Condition – Run 411. ....	45
32. Wave Spectra collected during Hurricane Camille Runs. ....	46
33. Plot of Significant Single Amplitude Roll in Sea State 8 – Hurricane Camille. ....	46
34. Plot of Significant Single Amplitude Pitch in Sea State 8 – Hurricane Camille. ....	47
35. Plot of Significant Single Amplitude Yaw in Sea State 8 – Hurricane Camille. ....	47
36. Plot of SSA Vertical Bow Acceleration in Sea State 8 – Hurricane Camille. ....	48

## TABLES

1. Comparison of Pre-Contract DDG51 as Compared to As-Built DDG51 and DDG79.....	49
2. General Conditions Performed for Model 5514, Pre-Contract DDG51 Capsize Test.....	49
3. Mass Properties End of Service Life Load Limit, Intact 100 kt Wind Limiting KG. ....	50
4. Mass Properties End of Service Life Load Limit, Righting Arm Limiting KG. ....	50
5. Rudder and Propeller Characteristics for Model 5514. ....	50
6. List of Model Data Channels and Calibrations for Model 5514.....	51
7. Wave Height Sonics Located on MASK Bridge. ....	51
8. Desired Wave Conditions as Defined by Test Matrix and Model Geometry. ....	52
9. Uncertainty Estimates for Instrumentation. ....	53
10. Regular Wave Settings for Model 5514 Capsize Experiments. ....	53
11. Summary of Roll Decay Roll Periods and Autopilot Coefficients, ....	54
12. Summary of Turning Diameter Maneuvers. ....	54
13. Summary of Zig-Zag Maneuvers.....	55
14. Run Matrix for Intact 100kt Wind Limiting KG = 8.55m, EOSL Load Condition.....	56
15. Run Matrix for Righting Arm Limiting KG = 8.22m, EOSL Load Condition.....	57
16. Roll Angle Matrix for Intact 100kt Wind Limiting KG = 8.55m, EOSL Load Condition....	58
17. Roll Angle Matrix for Righting Arm Limiting KG = 8.22m, EOSL Load Condition.....	59
18. Wave Matrix for Intact 100kt Wind Limiting KG = 8.55m, EOSL Load Condition. ....	60
19. Wave Matrix for Righting Arm Limiting KG = 8.22m, EOSL Load Condition. ....	62
20. EOSL Condition, Intact 100kt Wind Limiting KG=8.55m Test Versus FREDYN Results. ....	64
21. EOSL Condition, Righting Arm Limiting KG=8.22m Test Versus FREDYN Results. ....	65
22. Motions for Model 5514 in Storm Sea State 8 – Hurricane Camille, Fn=0.1. ....	66
23. Motions for Model 5514 in Storm Sea State 8 – Hurricane Camille, Fn=0.2. ....	67
24. Motions for Model 5514 in Storm Sea State 8 – Hurricane Camille, Fn=0.3. ....	68

## **ABSTRACT**

*The DDG51 pre-contract hull form as represented by Model 5514 was evaluated for capsize events at End of Service Life Load Limit for the Righting Arm Limiting and Intact 100 Knot Wind Limiting KG Conditions. The results are compared to FREDYN 9.3 predictions, and results from previous Model 5514 capsize experiments. Results are also presented for a limited number of calm water maneuvering and irregular wave test. The results are to be used as benchmarks for comparison with capsize results observed for future hull forms as compared to conventional hull forms.*

## **ADMINISTRATIVE INFORMATION**

This work was conducted at the David Taylor Model Basin, Naval Surface Warfare Center, Carderock Division (NSWCCD) by the Seakeeping Division (Code 5500). The work was funded by Naval Sea Systems Command (NAVSEA), PMS500, under Program Element 64300N. The work was performed predominately under work unit 05-1-5500-616.

## **ACKNOWLEDGEMENTS**

The authors would like to acknowledge the contributions of Scott Percival, Dave Schwartzenberg, Paco Rodriguez, Gordon Minard and Dennis Ralston in the initial preparation of the model. The authors would like to acknowledge the effort of Rielly Conrad in establishing ballast conditions from SHCP and Wah Lee in creating test matrix conditions from FREDYN predictions. The authors would like to acknowledge the fine photographic support of Martin Sheehan and Billy Boston for video support during and after the test. The authors would like to thank Matt Powell, Joe Kim, Tim Smith, Jose Tejada, Lloyd McCoy, Eric Christensen, Bob Sarbacker, Larry Mulvihill, Charles Turner, Floyd Farmer, and Brian Young for assistance during testing. The authors would like to thank Michael Hughes, Rachel Jessup, Will Frank, Beverly Simon, Justin Pollack, and Tim Smith for post test analysis.

## **INTRODUCTION**

The DDG51 pre-contract hull form as represented by Model 5514 was evaluated for capsize risk as a baseline comparison to results currently observed for new hull concepts. The pre-contract DDG51 differs from the fielded DDG51 and DDG79 for the primary characteristics listed in Table 1. Generally speaking the DDG51 pre-contract hull is slightly wider (2.7 feet) and slightly shorter (17 feet – LOA) than the as built DDG51 and DDG79. The pre-contract DDG51 was ballasted to the maximum displacement allowed by End of Service Life (EOSL) Load Limit as defined by the service life percentage margins. The model was ballasted to two KG conditions as defined by Righting Arm Limiting KG and Intact 100 knot Wind Limiting KG per the Ship Hull Characteristics Program (SHCP) analysis output. The model as observed during capsize testing is shown in Figure 1. The model was built up to the Level 01 of the hull. It was tested in regular wave capsize conditions and some limited irregular wave storm conditions. The matrix of tests performed with this hull is provided in Table 2. Limited maneuvering data were collected for comparison to FREDYN simulations.

The ballast conditions for the model were determined by Ship Hull Characteristics Program (SHCP) analysis of the DDG51 pre-contract hull form. In working with the weight and arrangements for the DDG51, the EOSL conditions were evaluated based upon DDG51 end of service life weight growth criteria. The KG and roll metacentric characteristics were determined from SHCP analysis.

The model was ballasted and inclined prior to testing. Roll decay experiments were performed to further verify ballast conditions and to define autopilot coefficient settings. The model was tested for regular Wavelength ratios ( $\lambda/L$ ) of 0.75, 1.00, 1.25, and 1.50, and wave steepness ratios ( $H/\lambda$ ) of 1/10 and 1/15. These wave conditions were based upon predicted capsize events observed by FREDYN. The model was also tested in irregular wave conditions for a storm spectra in order to make comparisons of motion statistics and stability issues observed for other hull forms operating in the same storm spectra.

## **MODEL DESCRIPTION**

Model 5514 is a 1/46.6th scale model previously constructed at Carderock Division, Naval Surface Warfare Center (NSWCCD) model shop. The model was cast from a mold which previously NSWCCD had obtained from the Massachusetts Institute of Technology. The model



was constructed in 1996 in support of early capsize testing performed at NSWCCD as described by Thomas and Hoyt<sup>1</sup>.

### **Hull Configuration**

Model 5514 is built as a fiberglass model with Stereo-Lithographic Apparatus (SLA) bilge keels and rudders. Due to the fact that only EOSL conditions would be tested, there were a decent percentage of model components and ballast weights that could be moved to satisfy ballast test conditions. However, the model had to maintain watertight integrity, allow for battery change outs, and internal access for switching on and off of electronic circuits as well as allow space top-side for antennas and the metacentric height adjustment pole. Hence the bigger issue was the balance between space claims and satisfying ballast conditions. The general model layout can be seen in photographs provided in Figures 2 and 3. Turbulence stimulation for the model was provided by a series of studs ( 0.13" dia x 0.12" high) at approximately 0.6 inch spacing along the circumference of the bow bulb, in a line parallel with the leading edge of the bow but approximately 5 inches aft of the bow, and at the circumference of Station 5 up to an inch or so above the waterline.

During model outfitting, the weight and location of each component was meticulously logged so as to determine its contribution to the models' final center of gravity and inertial characteristics. Once the fixed components were located in the model as required by mechanical and instrumentation needs, the model was weighed and initial ballast conditions were measured. This was accomplished by performing an in-air center of gravity (CG) and gyradius measurement by attaching the model to the "A-Frame" inertial gear in a pendulum type fashion. The initial longitudinal CG is determined with this gear by knowing the amount and position of weight required to set the model at near zero pitch. The vertical CG is determined by adding or shifting weights and noting the change in trim. The vertical center of gravity (VCG) is determined by resolving the associated force diagram as the model CG swings under the pivot to offset the trim weight. The inertial characteristics are determined by measuring the roll and pitch periods of the suspended model once the CG has been determined. The roll and pitch inertias are then calculated based upon pendulum theory and application of the parallel axis theorem. The locations of movable weights and components were calculated in spreadsheet fashion to satisfy required ballast conditions. This whole process was performed multiple times until the measured ballast condition satisfied the desired ballast conditions. The results of the ballast effort are presented in the ballast sheets shown in Tables 3 and 4. All model scale achieved ballast

---

<sup>1</sup> Thomas, William L. III and Hoyt, John G. III (2001). "Capsize Experiments of a Destroyer Hull Represented by Model 5514", NSWCCD-50-TR-2001/004. Distribution authorized to DOD and DOD Contractors only. Critical Technology (January 2001). Other requests shall be referred to Commander, Naval Sea Systems Command, 2531 Jefferson Davis Highway, Arlington, VA 22242-5160.

conditions were within two percent of the desired conditions with the exception of roll gyradius for the intact 100-kt wind limited KG. Due to geometry and weight constraints it was not possible to satisfy the KG and  $GM_T$  to the desired accuracy and at the same time satisfy the roll gyradius. Since the  $GM_T$  was thought to be a greater factor in the accuracy of the experiment, this was chosen as the value of most importance. The resultant accuracy of the roll gyradius was 7.5% greater than desired. Any components which were removed from the model in order to attach the hull to the “A-frame” gear were mathematically added to the ballasted hull system by calculating the added weight and inertial characteristics for each piece. Only two items were required to be added to the ballasted hull in this fashion – the “GM pole” and its weights.

The final part of the ballasting process involves measurement of the model’s transverse metacenter ( $GM_T$ ) as determined by an inclining experiment. To aid in fine adjustment of the model’s metacentric height, a “GM pole” is attached to the capsized model as shown in Figure 3. The pole is typically placed at the transverse and longitudinal center of gravity of the model so that as the GM is adjusted by shifting weights up or down on the pole, there is minimal effect on transverse and longitudinal CG, and pitch gyradius. There is however significant interplay between roll gyradius, vertical CG, and  $GM_T$  such that multiple iterations are often required to balance these values and meet the targeted  $GM_T$  conditions when shifting weights on the “GM pole”. The calculated GZ curve for model 5514 including watertight areas up to Level 01 is presented in Figure 4. This GZ curve is used in later dynamic stability analysis to determine righting capabilities at various angles of roll.

### **Model Propulsion and Control**

The model was fitted with propellers having approximately the same diameter and area ratio and same rotation direction presently on the as-built DDG51 ship. The DDG51 propellers were approximated with “commercial off the shelf” aluminum four bladed mixing propellers. Comparison between the fleet DDG51 propeller and the model scale propellers is provided in Table 5. The rudders were sized to match the size and location of the as-built DDG51 rudders, but designed to match the geometry of the Model 5514 hull for the rudder shoe. The model geometry constraints due to existing propeller locations and rudder shaft locations from previous testing dictated a rudder with slightly less chord and slightly more span than that of the existing full scale rudder. However the lateral area of the as-built DDG-51 rudders were equal to the model rudders used for this test as shown in Table 5. The general layout of the propeller and rudders is presented in Figure 5. Note that turbulence stimulation (sand) was provided on the leading edge of the rudders.

The model was powered with a single Aerotech BM-200 hall-effect brushless motor. Two right angle gear boxes were used to connect and rotate both propeller shafts with the one motor.

The motor was powered with two battery packs (32 VDC nominal) in series to provide an approximate buss voltage of 64 VDC. The motor was controlled with an Advanced Motion Controls B40A8Q hall effect motor controller. The 0-5 VDC control signal was provided by the on-board computer (OBC). The propeller shaft rotation was measured with an optical sensor triggered by reflective tape on an enlarged hub attached to an open end of the starboard right angle drives.

The rudders were mechanically linked to steer at the same angle and rate. The rudder linkages can be seen in the stern view of Figure 2. A push rod was attached to a rotary actuator and potentiometer forward of the aft deck step down. The rotary actuator was powered with a 32 VDC instrument battery and was controlled by an Advanced Motion Controls 25A8K motor controller. Feedback monitoring and control of the rudder system was also provided by the OBC and signal conditioning unit.

### **Instrumentation, Information, and Intelligence Control**

The instrumentation on the model consisted of several interrelated systems - the model power and control systems, the motion sensing instruments and their associated powering and signal conditioning electronics, the on-board computer, and the ArcSecond surface tracking system. The model propulsion motor and steering system were powered and controlled as described previously. The instruments, associated electronics, and on board computer were powered with a separate instrument battery (32 VDC). The tracker system needed to be isolated electronically from other model systems so that radiated electronic noise from motors and nearby circuits would not interfere with the low powered tracking system output signal. The tracker was powered by a separate 12 VDC battery. Four separate switches, located inside the hull near access panels on the model, energized circuits for the motor, the OBC and instruments, the roll and pitch gyros, and the tracker system.

The OBC was used to control the model and collect data. Input to the OBC were signals from motion sensing instruments, sensors collecting control and status of systems on the model, and instruments measuring model or environment data associated with the test. A photograph of the OBC mounted in the model can be seen in Figure 6. Visible in the figure are the RTD IDAN PC104 computer (on the right) and the National Instruments™ CB68LP analog I/O interface boards (on the left). Below the interface boards are four 8-channel filter boards configured for insertion of fixed low pass filters - in this case having a low pass filter rate of 12 Hz. The boards are populated with Frequency Devices Model DP78 Low Power 8-Pole Bessel filters. The OBC communicates in real time with shore based computers over an 802.11b or Wi-Fi network from a wireless Workgroup Bridge on the model to an Access Point associated with an isolated local area network onshore. Prior to output over the wireless network, the OBC Ethernet stream is

merged with the tracker data stream via a switching box. The tracker system will be described later.

The OBC data transmitted from the model are unpacked, collected, and stored in onshore computers. A remote laptop computer, configured with a virtual driver control console, allows for remote monitoring and control of the model. This laptop computer monitors the same data stream as is stored for data collection, but is restricted to presenting information on control systems to a LabView™ based driver control console displayed real-time on the computer's screen. A second shore-based computer unpacks the data stream and stores the model and control information as collected data only. The tracker system data is also unpacked and saved using tracker specific collection software.

The tracker system used for these tests was an ArcSecond Constellation 3DI Indoor GPS system. This system consists of six shore based transmitters rigidly mounted at fixed locations around the basin and the model based detector and associated electronics. The shore transmitters act like fixed indoor satellites providing a reference for locations within the basin. The transmitters have rotating heads which generate two infrared laser fanned beams and infrared LED strobes. The two fanned laser beams are tilted with respect to the axis of rotation, nominally negative 30° and positive 30° with respect to vertical. The head of each transmitter rotates at slightly different speeds centered around an operating speed of 40Hz. The model mounted detector can thus determine the transmitter reference based upon head rotation speed.

Vertical angle relative to each transmitter is calculated by knowing the angles of the fan beams, determining the difference in timing between the arrival of laser fan beam 1 and 2 at the detector, and finally knowing the speed of rotation of the transmitter head. Since the laser fan beams are tilted relative to vertical, the vertical location relative to the transmitter can be calculated. The measurement of the horizontal angle relative to a transmitter requires a horizontal index. This is accomplished when the transmitter fires an LED strobe at the same angular point in the rotation of the transmitter head. The detector also notes the passing of laser 1 and 2. By knowing the timing between the LED strobe, laser 1, and laser 2, the detector can determine the horizontal angle relative to the transmitter. Once the vertical and horizontal angle for a detector relative to a transmitter is known, the distances can be calculated based upon the transmitter geometry and other calculated angles relative to other transmitters. This calculation process is performed by a position calculation engine (PCE) electronic box associated with each detector. The PCE produces a serial stream for each detector indicating values measured relative to each transmitter and relative quality or "metric" of the information noted. The PCE serial stream is converted to Ethernet format and merged with the OBC output data stream via a switching box. The data sent to shore is received, unpacked, and handled with tracker specific software provided by ArcSecond and modified slightly with in-house programming.

The primary purpose of these model tests was to measure and define the motions, accelerations, operational conditions, and spatial parameters associated with the model as it operates in various capsize and seaway conditions. This measurement and documentation is accomplished using various specific instruments. A list of instruments installed in the model is presented in Table 6. The shaft RPM was measured using an optical sensor which detected pulses from a shaft hub marked with reflective tape. The pulses were converted to voltage by a frequency to voltage converter mounted on a custom circuit board. The rudder angle was measured by a rotary potentiometer. The model heading was measured with a fluxgate compass. Roll and pitch angle were measured by a vertical gyro. The three angular rates were measured using an angular rate sensor. All accelerations were measured with Columbia tri-axial mass accelerometers. The battery voltage for the instrument circuit was measured using a voltage divider which reduced the battery voltage by a factor of 3.3 for input to the OBC. Many of the model instruments can be seen in Figures 1, 2, 3, and 6.

All of the computers involved in data collection were time synchronized using an ESE-102 GPS master clock and a small time sync program linking all over the network. This system provided consistent time stamps for all data files collected.

## **FACILITIES**

All tests were conducted in the Maneuvering and Seakeeping basin (MASK) at Carderock Division, Naval Surface Warfare Center located in Bethesda, Maryland. Model preparation and outfitting was performed in the electronics and mechanical rigging areas of the MASK building. Model ballast conditions were obtained and verified using the A-frame inertial measurement gear and by performing incline experiments on the model in local ballast basins. Roll decay experiments were performed under the carriage of the MASK. All other free running model experiments (including speed calibration, stability, seakeeping, and maneuvering tests) were performed in open areas of the MASK basin.

### **Test Basin**

The DDG51 pre-contract capsize experiment was carried out in the MASK Basin as shown in Figure 7. The MASK is an indoor basin having an overall length of 360 feet, a width of 240 feet and a depth of 20 feet except for a 35 feet deep trench 50 feet wide parallel to the long side of the basin. The basin is spanned by a 376 feet bridge supported on a rail system that permits the bridge to transverse to the center of the basin width as well as to rotate up to 45° from the centerline as seen in Figure 7. With such a basin geometry, assuming transverse hull symmetry, a towed model can be exposed to all headings relative to the waves. A towing



carriage is suspended under the bridge on wheels. The motor driven carriage can traverse the basin at a maximum speed of fifteen knots.

### **Wave Generation and Measurement**

The MASK basin has eight pneumatic type wavemaker units located along the 240-foot side of the basin and thirteen units along the 360-foot side of the basin. Each bank of wavemakers can be operated individually or in unison. Wave height measurements were made from several fixed ultra-sonic level metering devices mounted on the MASK bridge. The approximate locations of the wave height sensors on the bridge are illustrated in Figure 7. The wave measurement channels are defined in Table 7. For all capsize and irregular sea test runs, the bridge was rotated to a thirty degree position across the basin. This was done to ensure better wave height measurement coverage of the portion of the basin typically used during testing. The approximate location of the bridge sonics when at thirty degrees is shown in Figure 8.

A desktop computer was used to generate the necessary input signal that would drive the wavemakers to reproduce a given random wave energy spectra. The computer generated, digital control signal sequences were applied to the wavemakers through a digital to analog (D/A) converter. The software used to generate the digital control sequences used a filtered white noise technique in the time domain to develop the spectra of interest. The long-crested irregular wave storm conditions specified for these tests was the spectrum collected in the Gulf of Mexico during passage of Hurricane Camille in 1969 – a measured storm spectrum. For regular wave operation of the wavemakers, a frequency generator input the prescribed sinusoidal drive signal to the wavemakers. The pneumatic blower motor speed (RPM) and pneumatic dome lips were altered as required to produce the waves of interest.

### **Tethered Carriage Operation**

During execution of the roll decay experiments, the model was loosely restrained under the MASK carriage with nylon cord. The nylon cord served to restrain the model during acceleration and deceleration phases of a carriage run, and served as a safety line for those cases when the model heading was not maintained in line with the carriage at speed. The cord was slackened during the data collection phase of a roll decay test run. The model was free-running for all other test conditions.

### **Free Running Model**

For speed calibrations, maneuvers, capsize runs, and seakeeping runs, the model was free-running (on battery power) without any lines or restraints. Support staff towed the model to a central location in the basin to begin start-up procedures and system checks. Once the model is fully operational, the support staff retired to a launch site in the corner of the MASK basin between wavemaker banks. At this point all control, tracking, observation, and data recording of

the model was done from remote locations. The model operator was typically stationed at an elevated window above the basin in the wavemaker control room for best viewing of the model and basin wave conditions. Experiments were performed as described by the Experimental Procedure. Support staff in the punt retrieved, inspected, and oriented the model as required.

### **Tracking System**

Whenever the model operated as a free-running model, its position was tracked in the basin using the ArcSecond Tracker system described earlier. The theory of operation and components of the onboard sensor and shore based tracking system are described in the Model Description section of this report. Shore based computers processed tracker data received from the model and displayed a visual representation of the track of the model for each test run. This hull was fitted with a single detector due to weight and space limitations on the model. Up to three detectors have been employed in other hull models.

## **EXPERIMENTAL PROCEDURE**

In order to verify model and wave field characteristics, several preliminary procedures were conducted in preparation for testing. These preliminary steps consisted of determining regular and irregular wave settings, measuring roll decay characteristics of the model, determining speed settings of the throttle control, and documenting model maneuvering characteristics. Once the preliminary procedures were completed, the free-running capsize regular and irregular wave runs could be completed as described below.

### **Wavemaker Settings**

Prior to testing the model it was first necessary to determine the wavemaker blower RPM and dome lip immersion settings required to generate the wave conditions as defined by the test matrix presented in Table 8. A historical database of blower RPM settings for the various wave frequencies of interest exists, however due to the many variables and non-linearities of the wavemaking system, it is best to verify the blower RPM settings prior to each test. For stability tests, the wave calibration process begins by setting the bridge at thirty degrees in order to maximize wave sonic coverage as shown in Figure 8. The wave frequency is set, and the initial blower RPM input and executed by the wavemaker operator. Wave elevation data is recorded for the six active bridge sonics. A harmonic analysis is performed to determine the average wave field statistics for that RPM setting. Statistical outliers are not included in the average. This process is continued for all of the prescribed wave conditions until RPM values are determined for each wave.

### **Roll Decay**

Calm water roll decay tests were performed at Froude numbers ( $F_n$ ) of 0.0, 0.1, 0.2, 0.3, and 0.4. The tests were performed using the MASK carriage to accelerate the model to the desired speed. Restraining lines connected the model to the carriage. A pair of hydraulic cylinders on the east and west side of the carriage were used to loosen and tighten the restraining lines as required when the model reached the commanded speed during a test run. At  $F_n=0.0$ , with restraining lines loosened, the model was excited to roll by sharply depressing the midship gunwale (with a pole) and then quickly releasing the model so that only the rapid release of the impulse force excited the model to roll. The model was allowed to roll until the motion amplitude decayed to below  $1^\circ$ . At Froude numbers greater than 0.0, the model was accelerated to speed by the carriage and restraining lines. Once at speed, the lines were loosened. As directed by the model driver, the “pole man” would excite the model to roll. Again, the model would be allowed to roll until the amplitude decayed to below  $1^\circ$ . This process was done for both port and starboard gunwales, and for a range of initial release angles. Upon completion of a test run, the data was immediately inspected for quality and processed to determine the roll period of the model for that test condition. The roll period data were used as input to determine autopilot coefficient settings required to conduct the at speed stability and seakeeping experiments.

### **Speed Calibration**

The speed calibration is the process where by the throttle CMD voltage required to achieve a particular model speed is determined. For this process the model is free running in the basin. The MASK bridge is moved to the storage location at the south side of the basin. The model is driven in a clockwise fashion around the basin such that it is driven in a straight line parallel to the longbank wavemakers, approximately 20' out from the wavemaker. A pre-measured distance of either 50' or 100' along the north shore is used as reference distance across which the model is timed to determine model velocity. This is done at multiple throttle CMD voltages bounding the range of speeds ( $F_n$ 's) to be tested. When greater speeds are to be tested the 50' reference distance is used to ensure that the model has adequately accelerated up to a steady state speed along side the wavemakers. The throttle CMD voltages and propeller RPM are recorded and plotted versus measured speed. Once a suitable relationship curve is defined for the range of Froude numbers, the speed calibration is complete.

### **Maneuvering Runs – FREDYN Correlation**

The model test was performed to determine regular wave capsize events as noted by scaled model testing. Concurrently there is an on going effort to determine the suitability of the FREDYN program to accurately predict capsize events. Various aspects of FREDYN are being investigated, modified, and enhanced. To assist in this effort certain basic maneuvers were

performed in the MASK basin to provide correlation data as it relates to control surface movement and the corresponding model motions and track. Space limitations in the MASK prevent a complete array of zig-zag and turning circle maneuvers, but a limited number of conditions are performed to provide a small amount of data for correlation.

All maneuvers are performed in calm water conditions with the MASK bridge moved to the far south side of the basin. The model is first brought up to the desired speed as determined by the “speed calibration” process described above. The model is directed along the right heading and location required for the maneuver to be performed. Prior to maneuvers the rudder movement and yaw rate is minimized for the maneuver approach. For the turning maneuver the rudder is sent to the port or starboard angle of interest. The model is kept at that rudder angle until the model has completed one and a half turns ( $540^\circ$ ) of the turning circle. The turning maneuver is then terminated. This is repeated for both port and starboard executes. Turning maneuvers were performed for  $F_n=0.20$  with nominal rudder executes of  $10^\circ$ ,  $20^\circ$ , and  $30^\circ$ ; and for  $F_n=0.30$  with a nominal rudder execute of  $10^\circ$ .

The zig-zag approaches were accomplished in the same form as that described for turning circles. The zig-zags were performed manually for this test, meaning that the operator was responsible for noting the change of headings and hence when rudder executes should be performed. Only 10-10 zig-zags at  $F_n=0.2$  and  $0.3$  and 20-20 zig-zags at  $F_n=0.3$  were performed, with varying amounts of success. The 10-10 zig-zag is defined such that once the model is on an initial constant heading, the rudder is thrown to  $10^\circ$  to port or starboard. Once the model heading has changed  $10^\circ$  from initial heading toward the direction of steerage, the model rudder is thrown to  $10^\circ$  on the opposite side. Once the model heading has achieved a  $10^\circ$  deviation from initial heading on this new side, then the model steering is once again shifted to  $10^\circ$  of rudder on the opposite side. This process is repeated until basin space is no longer adequate. For the 20-20 zigzag the rudder executes are  $20^\circ$  and the change of heading to initiate executes is also  $20^\circ$ .

In some previous remote control models the zig-zag maneuver has been programmed into control computers or set up with voltage standards for plus and minus steering angles. Unfortunately at the time of this test, this maneuver had not yet been programmed into the OBC or shore based control computer. A programmed maneuver would greatly improve the quality of the zig-zag maneuver due to the quick response time required to execute the steerage angles based upon the rapidly changing headings. However space limitation of the MASK will always be the limiting factor in obtaining top quality zig-zag data in the basin.

### **Regular Wave Capsize**

The purpose of the test is to run the model in regular wave conditions as identified by the FREDYN analysis to determine capsize occurrence. As such the wave conditions defined by the Wavemaker Settings effort, and the throttle command defined by the Speed Calibration effort will be employed for the regular wave capsize conditions.

The autopilot coefficients are set into the autopilot algorithm based upon the Froude number at which the model will be operated. The model is brought via the punt crew to the launch location. For headings 0° and 15° the model is held and released via a stern, string launch from the short bank wavemaker catwalk. For headings 30° through 60° the model is launched from the punt in the north-west corner of the basin. For headings 75° through 105° the model is launched from the punt while along the short bank wavemaker. The launch crew aligns the model to the proper heading and the model is restrained.

The wavemaker starts to produce waves. Once enough of the basin is established at the desired wave condition, the model is brought to the proper throttle command voltage and the model is released. The model accelerates to speed and the autopilot is initiated once it is clear that the model is not in any danger of running into the wavemaker. In some instances a “Turbo” mode is initiated to provide extra throttle required to accelerate the model away from the launch location.

Video collection, tracker data collection, and model data collection is initiated at different stages in this process in order to properly document the capsize runs. The video collection is initiated early in the sequence in order to document any problems which occur in the launch process. The tracker and data collection does not typically begin until right before the model launch, but generally occur at the same start point in the run. As the run progresses an observer other than the driver notes motions of the model, capsize risk events, and mechanisms which can or actually do cause a capsize.

Irregardless of achieved model speed or heading, the observations and data are assigned or scored to the wave conditions and model speed and heading defined by the initial target conditions. The run is terminated when an actual capsize occurs, or when there is no more running room in the basin, or when the model is unable to operate in the given seaway (cannot maintain speed/heading).

If the model exhibits high roll angles or other capsize risks, then multiple runs at that condition are executed. The runs are performed to determine consistency in the result, verify observed motions, and to determine if initial conditions play a factor in the observed results. The test crew determines that the results are of consistent quality and thoroughly documents the observed reaction to the defined initial conditions.



## **Irregular Wave Seakeeping**

Model 5514 was tested for dynamic stability in extreme storm waves only. The as-built DDG51 hull form has been a very good seakeeping performer. However to provide comparison to other proposed hull concepts, it was decided to test the pre-contract DDG51 at EOSL conditions. The scale ratio 46.6 Hurricane Camille storm spectra had been previously developed for other equally scaled capsized models. For the irregular wave test the model is run as a free-running, remotely controlled model. The model is placed in the basin. In the event of model mishap or capsize the punt crew stays in standby mode on shore. The wavemaker is run to fully establish the irregular wave environment.

The model is maneuvered in what is often referred to as a racetrack course. The model is maneuvered to the correct heading and set on autopilot. Once on heading and at speed the driver calls for video and data collect. The video, tracker, wave, and model data is collected until the driver calls for the end of the run. The run length is determined by the driver based upon the space required to turn the model about for the opposite 180° heading. This technique results in data sets such as 0° and 180°, 90° and 270°, and 150° and 330° being collected concurrently on alternating runs. It should be noted that transverse symmetry is assumed for the model such that the mirror image of wave effects on the port side would be assumed for the starboard side (i.e. 30° would be assumed equivalent to 330°, 60° equivalent to 300°, 120° equivalent to 240°, etc.). This procedure is continued until approximately 30 minutes of full-scale equivalent data is collected.

## **UNCERTAINTY ANALYSIS**

Uncertainty analysis as applied for this report is based upon the ISO Uncertainty Guide [1]. The analysis consists of two parts: (1) Type A evaluation and (2) Type B evaluation. For this report, all uncertainties are defined at the 95 % confidence limit. The Type A is computed from the time series data,  $x_k$ , acquired during at test and is defined as follows for the mean value:

$$u_A = k\sigma_x / \sqrt{n} \quad (1)$$

where the standard deviation of  $x$  is

$$\sigma_x^2 = [1/(n-1)] \sum_{k=1}^n (x_k - \langle x \rangle)^2 \quad (2)$$

and the mean of  $x$  is

$$\langle x \rangle = (1/n) \sum_{k=1}^n x_k \quad (3)$$

where  $n$  is the number of samples and  $k$  is the coverage factor and  $k = 2$  at the 95% confidence level. Typically, these experiments were highly unsteady and random in character, and the

standard deviations were not typically computed. Consequently, most of the uncertainty was determined by Type B evaluation method.

The Type B uncertainty was determined from calibration of the instruments. For most electronic instruments, the uncertainty in the reference standards is small in comparison to the uncertainty in the electronic transducers. For conversion of the voltages from the A/D converter in the data acquisition system to engineering units or physical units, the slopes and intercepts from regression analysis of the calibration data were applied to the data. The uncertainty was determined by calibration theory from Scheffe [2] and Carroll, et al.[3].

The results of the uncertainty estimates are summarized in Table 9. The table includes an example calculation of the Type A uncertainties during a steady state run DDG-51-0371 on smooth water for calibration at maximum model speed, 2.22 m/s ( $Fn = 0.407$ ). As the table indicates the Type A uncertainty estimates are small in comparison to the Type B.

The Type B uncertainties vary with the value of the calibration reference value; however, the result is nearly constant in physical units. The maximum values are indicated in Table 9.

For those quantities not measured directly such as Froude number and non-dimensional wavelength and height, the uncertainties were propagated with the following equation for the combined uncertainty [1]

$$u_c^2 = \sum_{i=1}^N [(\partial f / \partial x_i) U(x_i)]^2 \quad (4)$$

### **Acceleration**

Accelerations were measured at the bow, stern, and CG (center of gravity) of the model. Acceleration was referenced to local g (local acceleration of gravity) via a tilt table with a resolution of 10 minutes of arc. Example plots of the residuals in the calibration of vertical and transverse accelerations at the model CG are shown in Figure 9, where the residuals are defined as the differences between the data and the straight line fit from linear regression analysis. The dashed lines are the calibration uncertainties at the 95 % confidence limit from statistical calibration theory. From Chauvenet's criteria [4], outliers occurred at mid-range in the transverse bow accelerometer and in the stern transverse accelerometer. These outliers, slightly outside the 95% confidence limit, were not excluded from the calibration data. However, an outlier at +1g in the CG longitudinal accelerometer of Figure 9a was removed from the calibration data since an acceleration of +1 g was not expected.

Due to the method of calibration, the vertical accelerometers responded only to negative values for g. To improve statistical sample size, the calibration procedure was repeated for these transducers. Consequently, much of the uncertainty in their calibration can be attributed to a hysteresis effect as indicated in Figure 9b.

Local gravity in absolute units from Moose [5] is  $9.80101 \pm 0.00004$  m/s<sup>2</sup>

( $32.1555 \pm 0.00013 \text{ ft/s}^2$ ). This value was computed from the web page

<http://www.ngs.noaa.gov/TOOLS/Gravity/gravcon.html>

for a latitude of  $38^\circ 58' 36.69''$  and longitude of  $77^\circ 12' 4.96''$  (center of the MASK basin). For all calculations on this project, standard g has been applied,  $9.80665 \text{ m/s}^2$  ( $32.17405 \text{ ft/s}^2$ ), which implies an error in application between standard g and local g of 0.058 %.

### **Pitch and Roll Angle**

Pitch and roll angle were measured with a Humphrey (now Goodrich Rosemount Aerospace) vertical gyro, which was calibrated on a tilt table having a resolution of 10 minutes. The results for roll calibration are shown as a residual plot in Figure 10. No outliers were observed in roll angle, but one was observed in pitch at  $-50^\circ$ . The outlier was removed from the analysis for calculation of the final calibration constants.

The data in Figure 10 are from a post-test calibration, where the reference angle was measured by an Applied Geomechanics Pro 3600 Digital protractor with a resolution of  $0.1^\circ$ . The gyro was not properly calibrated before the test. The slope in Figure 10 ( $-10.678^\circ/\text{V}$ ) shows that the post cal was 0.66 % lower in magnitude than the calibration factor applied during the test ( $-10.749^\circ/\text{V}$ ). For pitch angle, the pre- and post cal slopes were  $+7.129$  and  $+7.151^\circ/\text{V}$ , respectively. By a statistical hypothesis test, the pre- and post-cal slopes for pitch angle were considered identical.

### **Model Velocity and Propeller Shaft Speed**

The throttle CMD voltage data channel, an indicator of shaft RPM, was used to set Model velocity for these tests. As previously stated, the shaft speed was detected by an optical sensor and converted to a voltage by a frequency to voltage converter. The results of the calibration for shaft speed are presented in Figure 11. The calibration process involved simulating shaft RPM using a function generator as input to the frequency to voltage converter. Type A uncertainty is displayed in Figure 11 by error bars. It should be noted that the magnitude of the error bars displayed for other data channels were typically smaller than the size of the symbols used to plot the data.

The data displayed in Table 9 is derived from this calibration. Type A uncertainty (as measured at the maximum model velocity during calibration run DDG-51-0371) is shown in the table. Table 9 indicates that Type B uncertainty dominates this process. The total uncertainty in shaft speed is about  $\pm 3.6 \text{ RPM}$ .

The model velocity was computed by measuring the time for the model to pass basin markers spaced 100 ft (30.48 m) apart while maintaining a fixed shaft RPM. Model speed uncertainty was then estimated from two methods - the calibrations of model speed versus shaft RPM and model speed versus throttle CMD setting. The resulting model speed uncertainty

(from the two methods) over the Froude number range of interest was found to be  $\pm 0.13$  m/s ( $\pm 0.43$  ft/s) by the measured shaft speed method and  $\pm 0.54$  m/s ( $\pm 1.77$  ft/s) using the throttle setting method. Clearly, from inspection of these calculated results, the measured shaft speed produced a lower uncertainty in model speed. In recent tests for other propeller driven models, the measured shaft speed generated a lower uncertainty in model speed.

A significant reduction in model velocity uncertainty was obtained by using a second-order curve fit to the shaft speed calibration data. From statistical theory, the maximum prediction limit was found to be  $\pm 0.050$  m/s ( $\pm 0.16$  ft/s). The actual Froude number during a test should be computed with the measured propeller shaft speed using this second-order curve fit. The residual plots of the 1<sup>st</sup> and 2<sup>nd</sup> order curve fits are shown in Figure 12.

The variation in model speed can be estimated from the standard deviation of the shaft RPM by the Type A uncertainty evaluation method. An example estimate is provided in Table 9. In this case, the estimated uncertainty is  $\pm 0.9$  mm/s, which is negligible in comparison to the velocity calibration uncertainty.

As a check on the velocity uncertainty, the stopwatch results were compared to those recorded from the tracker. The velocity was computed from tracker points approximately 30 m (100 feet) apart that were acquired at the same time as the stopwatch data. The results of the difference between the data are presented in Figure 13. The mean difference was  $+1.8 \pm 45$  mm/s. Statistically, the difference is the same as zero. The uncertainty is also within the prediction limit of the velocity calibration as determined by the shaft speed from the 2<sup>nd</sup> order curve fit.

Correction of the stopwatch data for heading relative to the 30.48 m (100 ft) markers did not significantly affect the results. A  $\pm 5^\circ$  degree correction in heading using a cosine function correction factor resulted in only a  $\pm 0.4\%$  change in uncertainty.

Model speed for these tests was specified as a function of Froude number ( $Fn$ ), which is defined as

$$Fn = V / \sqrt{gL_m} \quad (5)$$

where  $V$  is the model velocity,  $g$  the local acceleration of gravity, and  $L_m$  the model length. The uncertainty in  $Fn$  was then estimated from eqs. (4) and (5) as

$$(u_c / Fn)^2 = (u_v / V)^2 + (u_g / 2g)^2 + (u_L / 2L_m)^2 \quad (6)$$

with the uncertainty in velocity,  $u_c$ , from Figure 12a, model length,  $L_m = \pm 2.5$  mm ( $\pm 0.1$  in.), and  $g$  as the difference between local and standard  $g$ . The influences of  $g$  and model length,  $L_m$  were considered nil. As such, the uncertainty in  $Fn$  was dominated by the velocity,  $V$ . For Froude numbers between  $0.1 < Fn < 0.4$ , the uncertainty in  $Fn$  was found to be  $0.019 < u < 0.024$ .



## **Heading**

Model heading was not calibrated. Manufacturer's specification of accuracy was stated as  $\pm 1^\circ$ . As a check on model heading, heading results from the model were compared to tracker results. The 30.48 m (100 ft) markers were assumed to have a heading of  $135^\circ$ . Since the coordinate system for the tracker was indexed to the basin,  $135^\circ$  was subtracted from the model heading results. This result was then compared to the heading from the tracker. The difference in the angle is presented in Figure 14. The average difference was  $-10.52^\circ \pm 2.22^\circ$ .

Statistically, the difference is not zero. Most of the difference may be in the assumed heading of the basin. If the difference between model and tracker headings can be resolved, the uncertainty in model heading would appear to be  $\pm 2.22^\circ$ .

## **Rudder Angle**

The rudder angle was calibrated with a protractor of unknown resolution and accuracy. The resulting calibration of rudder position as a function of voltage output from the rudder angle potentiometer indicates an uncertainty of  $\pm 0.80^\circ$  for the rudder at its limits of operation ( $\pm 30^\circ$ ). The measurement uncertainty in the angle determined by the protractor is assumed to be small in comparison. The residuals for the calibration are shown in Figure 15. One outlier of unknown origin was eliminated from the regression analysis.

## **Rudder Angular Rate**

The uncertainty in rudder angular rate was determined by computing the standard deviation of the maximum slopes of the rudder displacement trace for specified data runs. The rate, as determined from zigzag runs DDG-51-0171 through 0173 and DDG-51-0189 through 0183 - with model speeds between  $0.13 < Fn < 0.21$  and peak rudder angles of  $\pm 20^\circ$  - was estimated as  $64.7 \pm 2.6^\circ/\text{s}$ . This was considered statistically not the same as the design value  $68.3^\circ/\text{s}$  via a hypothesis test [5]. As a comparison, the rate was also computed from two regular wave runs (DDG-51-0216 and 0234) at  $Fn = 0.4$ . During these tests, the rudders were driven between  $-30^\circ$  and  $+30^\circ$  by the autopilot. The resulting rudder angular rate was calculated as  $66.0 \pm 1.6^\circ/\text{s}$  - which again is statistically not the same as the design value. However as a practical matter, the measured rate differed from the design rate by only  $2.2^\circ/\text{s}$  or 3.3 %.

The rudder rate uncertainty from the regular wave runs at  $Fn = 0.4$  is listed in Table 9. The uncertainty for rudder angular rate, as defined in the ISO Uncertainty Guide [1], was its repeatability. Zigzag runs were conducted under manual operation of the rudder, while during regular wave runs, the rudder was driven by an auto-pilot; consequently, the maximum rudder rate as determined under wave conditions may be a more reliable estimate of the maximum rudder angular rate.

Another estimate of rudder rate may be obtained from the calibration of the rudder angle. With the assumption that the timing uncertainty from the A/D converter is small in comparison



to the uncertainty in the angle, the estimated uncertainty is  $\pm 0.80^\circ/s$ , which is consistent with the previous estimate.

### **Wave Height Gage**

Wave height gages were calibrated relative to a calm water surface. This was accomplished by collecting data for each gage while supported at pre-set locations as determined by location pins spaced from  $-15$  to  $+15$  inches ( $-381$  mm to  $+381$  mm) in 5-inch (127 mm) increments above and below mean level on the gage staff. The estimated manufacturing tolerance of the pin locations was  $\pm 0.005$  inch ( $\pm 0.127$  mm). As an example, results of the residuals for wave gage calibration are presented in Figure 16 for wave gage #1. Four of the six gages (3, 4, 6, and 8) had one outlier each at wave heights of either  $+15$  inches ( $+381$  mm) or  $-15$  inches ( $-381$  mm). They occurred at the output limits of the probes (0 and 10 V) and were included in the slope calculations.

## **RESULTS**

### **Waves Settings**

The results of the wave calibration effort are presented in Table 10. The pneumatic wavemakers, while not perfect, can yield consistent results assuming that the hydraulic drive cylinders of the pneumatic wavemaker valves have been tuned. The blower RPM, the lip settings of the domes, and the control signal can be documented. If the hydraulic cylinders are tuned to provide a consistent movement based upon the drive signal input to the amplifier, then all variables of the wavemaking system - barring environmental factors - are documented and can be repeated consistently. Atmospheric changes - in terms of the air density input to the blower system - can create variations in wave output, but this variation is a small factor in the overall wavemaker variability. If the waves are monitored as the test proceeds, this variability can be minimized with small adjustments to blower RPM. The wave conditions recorded for regular and irregular testing are presented within their respective sections.

### **Roll Decay**

Roll decay experiments were performed at Froude numbers of 0.0, 0.1, 0.2, 0.3, and 0.4. The results from the roll decay experiments are used to document the observed roll period of the model and calculate the roll decay coefficient for the model operating at a constant forward speed. Roll decay experiments were run for both KG ballast conditions at EOSL. The measured roll periods are presented in Table 11. The roll periods estimated by FREDYN are also presented in Table 11. The measured roll periods were used to determine heading and yaw rate coefficients for the autopilot algorithm. These roll periods are presented graphically in Figures 17 and 18. Predicted versus measured roll periods were generally within 0.5 seconds. The roll

periods were typically under predicted by FREDYN for KG=8.55m and over predicted by FREDYN for KG=8.22m. Estimated roll periods using Equation 173, of Principles of Naval Architecture, Volume III [7] are presented for the target ballast conditions and the achieved ballast conditions. The measured roll periods and the calculated roll periods (based upon achieved ballast) agree within 0.20 seconds.

The roll decay coefficients are presented in Figures 19 through 28. Roll decay coefficients are defined by the equation :

$$N = \frac{1}{\pi} * \ln \left( \frac{\phi_1}{\phi_2} \right) \quad (7)$$

where  $\phi_1$  and  $\phi_2$  are successive cycles in the roll decay time history. Hence the data presented uses the envelope analysis method where roll amplitudes are measured from peak to trough, or trough to peak. This avoids the effects on an inaccurate mean or “zero” roll value reference. Generally there appears to be very little difference between the two KG conditions. There is a lot of scatter in the roll decay coefficients, but the coefficients appear slightly greater for the GM=1.25m data due to the higher righting arm. For Froude numbers less than and equal to 0.2 there is a large variation of roll decay coefficient with respect to roll angle indicating non-linear roll damping. For Froude numbers 0.3 and 0.4 the roll coefficient appears more constant with respect to roll angle due to the effect of damping at high speeds.

### **Maneuvering**

The results of the maneuvering effort were of marginal quality. The maneuvering results are really only adequate for comparison to FREDYN simulations. The turning data is generally of decent quality as indicated by the analysis, but the zig-zag data are very scattered due to the quality of the maneuver execution. In the future, both of these maneuvers should be a programmed process executed by an on-board algorithm.

The results of the turning maneuvers are provided in Table 12 . Rudder angle values for the port and starboard executes were not always consistent, but plots of tactical diameter versus rudder angle (Figure 29), show that measured tactical diameters are very well behaved regardless of speed. Turning diameters for conventional displacement hulls are expected to be a function of rudder angle only and independent of speed. The biggest variable in the quality of the turning data is the steadiness of the approach and the scatter of the steady heel angle during the turn.

The results of the zig-zag maneuver are provided in Table 13. The number of runs is very limited, and the analysis required inventive piece-wise investigation. The model overshoot angles of Table 13 appear consistent for each particular configuration. A graphical example of the heading and rudder angle recorded during a zig-zag maneuver is presented in Figure 30. In addition to the issue of execution, the quality of the zig-zag maneuver was affected by space

limitations in the basin itself. The model would typically have space to perform only two or three rudder executes to each side before running out of navigable space in the basin. This would leave only one or two executes for zig-zag analysis before the run was terminated.

### **Dynamic Stability – Capsize Evaluation**

As previously stated, the primary purpose of this test was to define the dynamic stability and capsize characteristics of the pre-contract DDG51 hull form as a baseline comparison to proposed future navy hull forms. The test matrix to be evaluated was based upon FREDYN analysis of the particular hull configuration. The test matrix evaluated all FREDYN predicted capsizes. The final run matrix completed for the test is presented in Tables 14 and 15. The capsize conditions are presented as red cells, and any non-capsize but still high risk areas as indicted by high roll angles are presented as yellow cells. All capsize or risk oriented runs were analyzed by evaluating the time history of the run, and by verifying that parameters of the test conditions were correct and constant at the start of the run. Figure 31 displays a typical run time history in terms of data channels utilized to inspect and verify the run's quality. The proper RPM/speed setting and heading was verified and compared with the observed roll motions. The model must accelerate and reach a steady heading before the condition can be fully identified as being satisfied. Once this is verified in the time history, the model must run for a sufficient time at steady state prior to the final capsize or other observed phenomena.

Maximum measured roll angle was also used to quantify the capsize risk for the test condition. The maximum roll angles observed for each run are provided in Tables 16 and 17. The max roll angle for a multi-run cell will be in the same run order as observed for Tables 14 and 15. The roll angle for the point at which seventy-five percent of the GZ curve area has been expended is listed in the key of each table. This value has typically been a threshold at which capsizes are most likely to occur. Values of the actual wave conditions achieved during the test are provided in Tables 18 and 19. All wave conditions tested were within accepted limits of the desired targeted conditions.

The matrix comparison between FREDYN predicted capsizes and actual observed capsizes is provided in Tables 20 and 21. For the righting arm limited, EOSL conditions shown in Table 20, FREDYN had predicted 87 capsize events. Testing produced only eight actual capsize events and two hi-risk performance cells. For the intact 100kt wind limited, EOSL ballast condition (see Table 11), FREDYN had predicted 60 capsize events but none were observed.

Capsizes observed for the DDG51 were generally of one type - loss of stability resulting in high roll angle and capsize. In some near following headings (0° and 15°) this was caused by a surf and broach which would result in a dramatic change of heading ( $\geq 30^\circ$ ). This would ultimately expose the model to an increased risk of capsize. The loss of stability capsize

generally occurred at headings of 30° and 45°, though capsize at a heading of 60° was also observed for  $\lambda/L=1.25$ . It should be noted that all capsizes occurred at  $F_n=0.4$ . There were some high-risk areas for  $F_n=0.3$  at  $\lambda/L=1.25$  and a heading of 45° that resulted in a high roll angle and loss of stability, but no actual capsizes were observed.

### **Seakeeping**

The model was tested in the Hurricane Camille storm condition as represented by the spectral plots of Figure 32. As is the case for any random process there is some variation in the spectral estimates due to differences in the limited collection time, but generally the spectra observed was fairly uniform for the various headings. The model was evaluated for the storm seaway at  $F_n=0.1$  and 0.2 for head, following, bow quartering, stern quartering, and beam headings. This data are presented in Tables 22 and 23. For a more limited number of headings the model was also evaluated at  $F_n=0.3$ . This was done to see if incidents of surfing and broach at  $F_n=0.3$  could be observed. Data collected at  $F_n=0.3$  are presented in Table 24. It should be noted that since there are no Sea State 8 operational requirements, the data was not used for comparison to performance criteria.

The data for roll, pitch, yaw, and bow vertical acceleration is presented graphically in Figures 33 to 36. Bar graph plots at various speeds and heading are provided for easier interpretation of the tabled values. The increased roll damping and course keeping of the hull as speed increases is seen in the SSA Roll of Figure 33 (Headings 45°, 90°, and 135°) and the SSA Yaw of Figure 35. The increase pitch and bow excitation due to increased speed in bow quartering (135°) and head (180°) seas can be seen in Figures 34 and 36. There are some variations in these trends due to variations in seaway, but these general trends are of enough consistency to note.

## SUMMARY AND CONCLUSIONS

The pre-contract DDG51 hull is a very stable ship. The model was ballasted to maximum displacement indicated by End of Service Life and the worst possible righting arm conditions short of a damaged hull. The hull experienced eight capsize and two near capsize events at the Intact 100 kt Wind Limiting KG ballast condition ( $GM=0.91m$ ) and no capsize events at the Righting Arm Limiting KG ballast condition ( $GM=1.25m$ ). These values dovetail very nicely with the results of Thomas and Hoyt<sup>2</sup> where two capsize conditions and three near capsize conditions were observed for  $GM=0.97m$  and no capsizes were observed at  $GM=1.42m$ , even though the previous model test was ballasted to a lower displacement of 7,923 LTSW. The model performed well during storm seaways as documented by the seakeeping results. The motions were greater than those allowed for operational pitch, roll, and accelerations but the Sea State 8 Hurricane Camille seaway is not considered to be an operational environment. The model was never in danger of capsize for this seaway. Further comparison of the collected pre-contract DDG51 data will be provided in a recently completed DDG79 dynamic stability test program.

---

<sup>2</sup> Thomas, William L. III and Hoyt, John G. III (2001). "Capsize Experiments of a Destroyer Hull Represented by Model 5514", NSWCCD-50-TR-2001/004. Distribution authorized to DOD and DOD Contractors only. Critical Technology (January 2001). Other requests shall be referred to Commander, Naval Sea Systems Command, 2531 Jefferson Davis Highway, Arlington, VA 22242-5160.



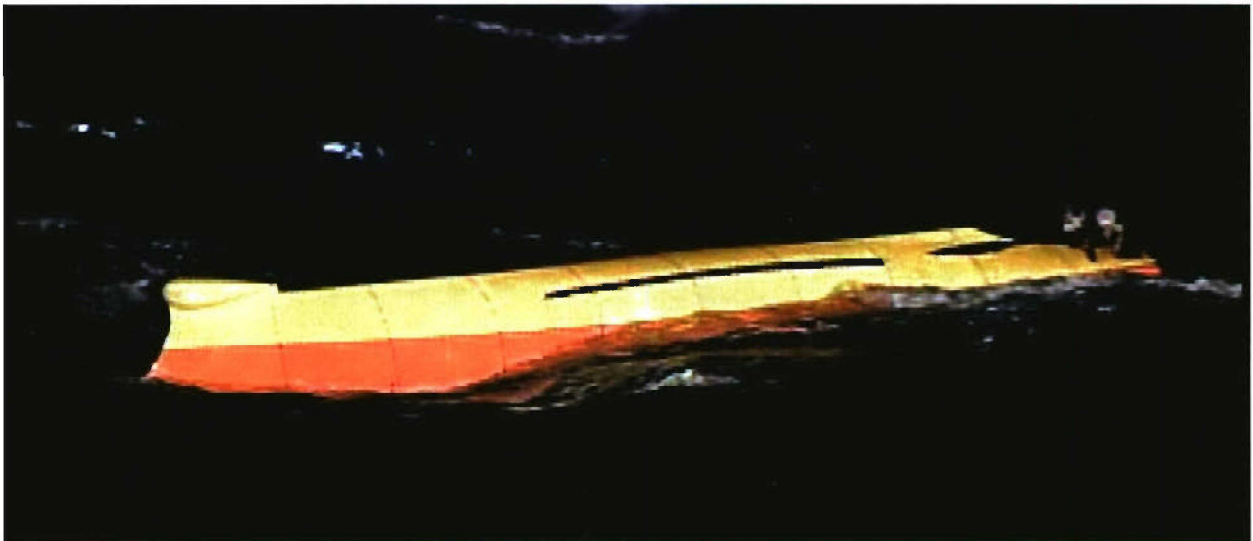
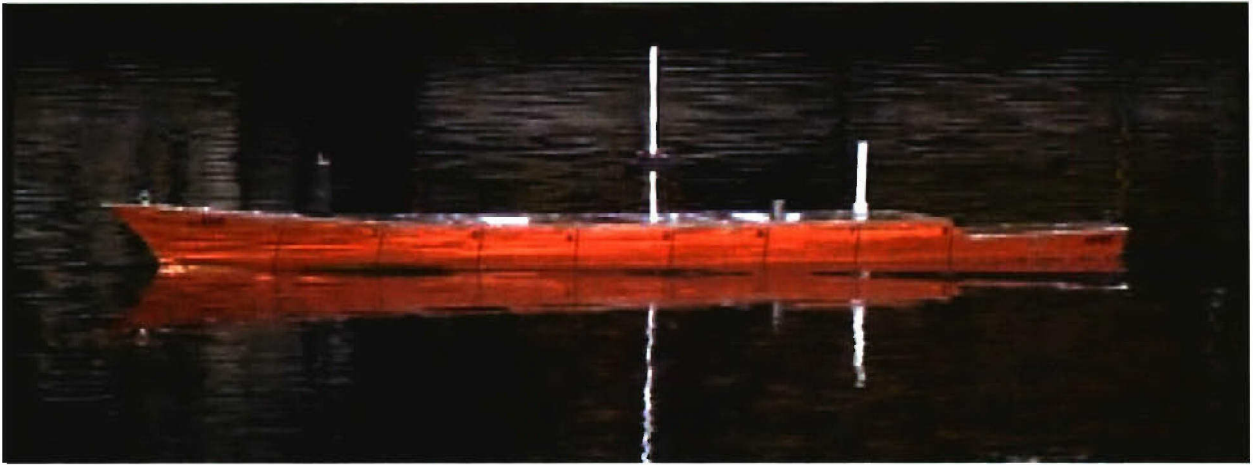


Figure 1. View of Model 5514 During Capsize Testing In MASK Basin.

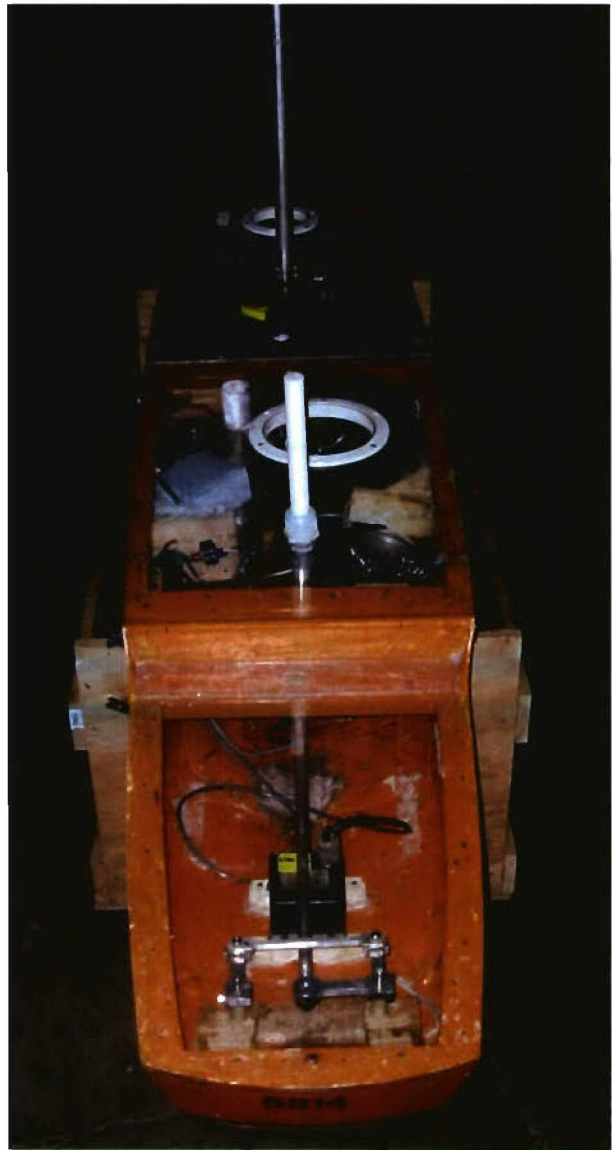


Figure 2. Model 5514 as Configured for Testing – Bow and Stern Top Views.



Figure 3. Model Arrangements at Mid-Ship Including GM Pole, and Battery Access Hatch.

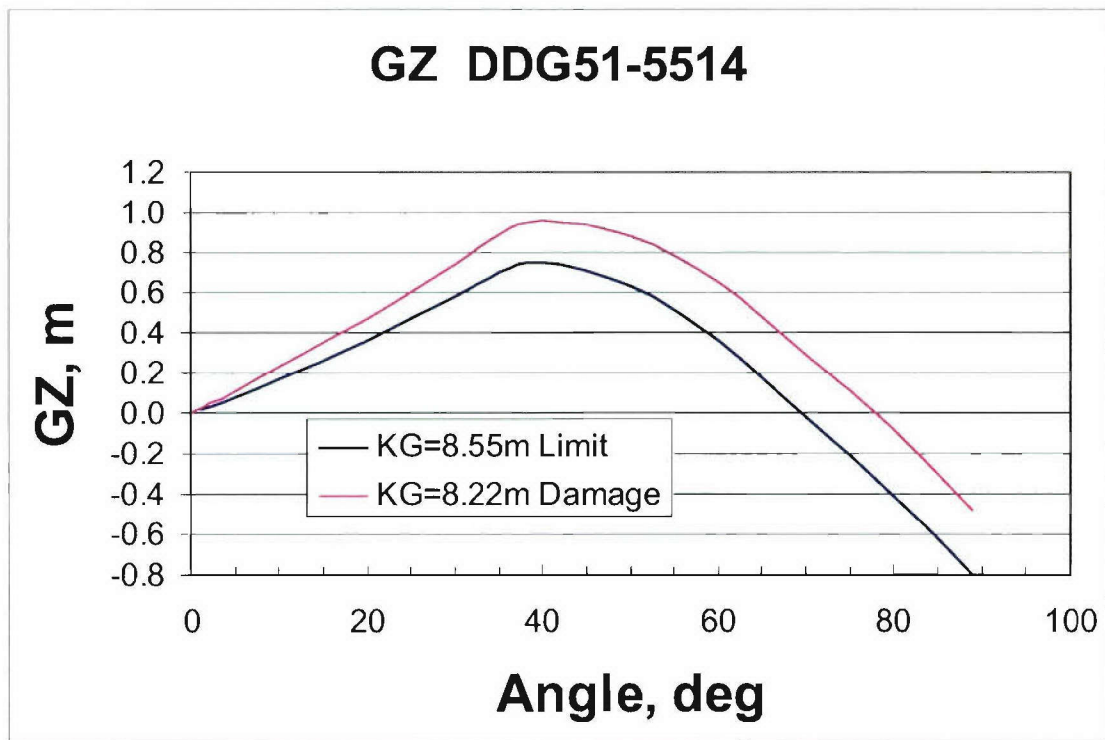


Figure 4. GZ Curve for Pre-Contract DDG51, Model 5514.





Figure 5. Propellers and Rudders for Model 5514.

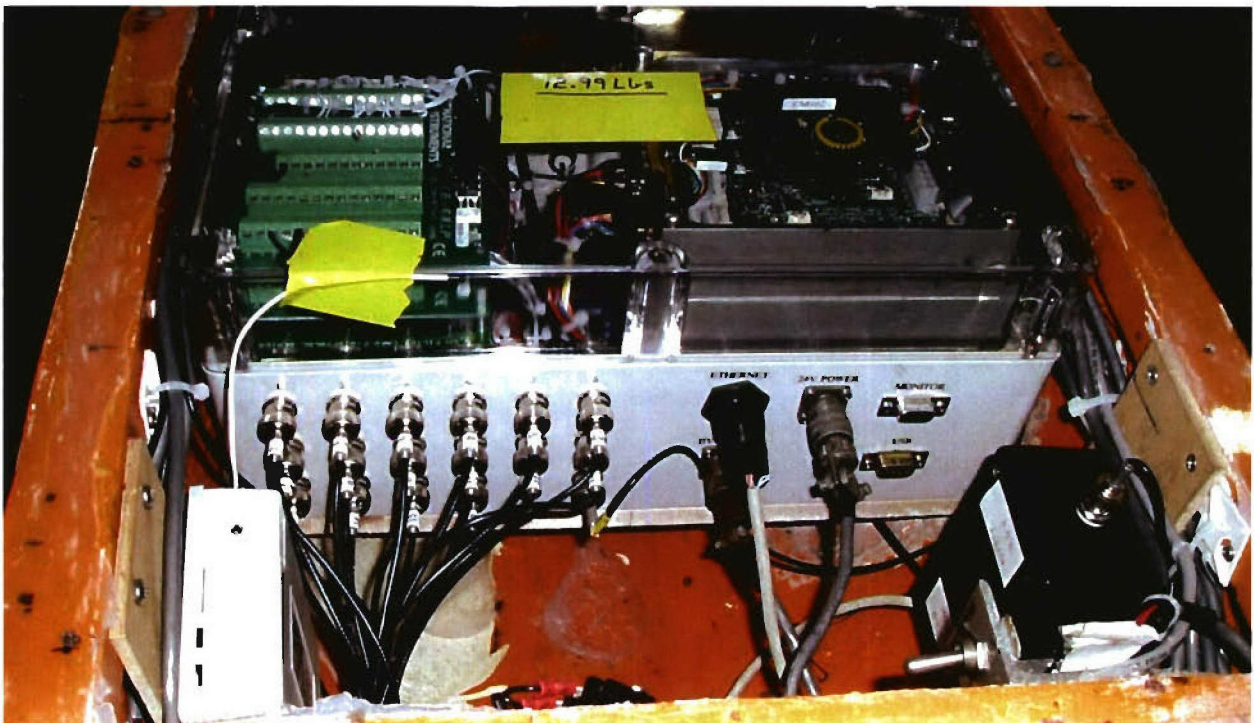


Figure 6. On Board Computer (OBC) of Model 5514.

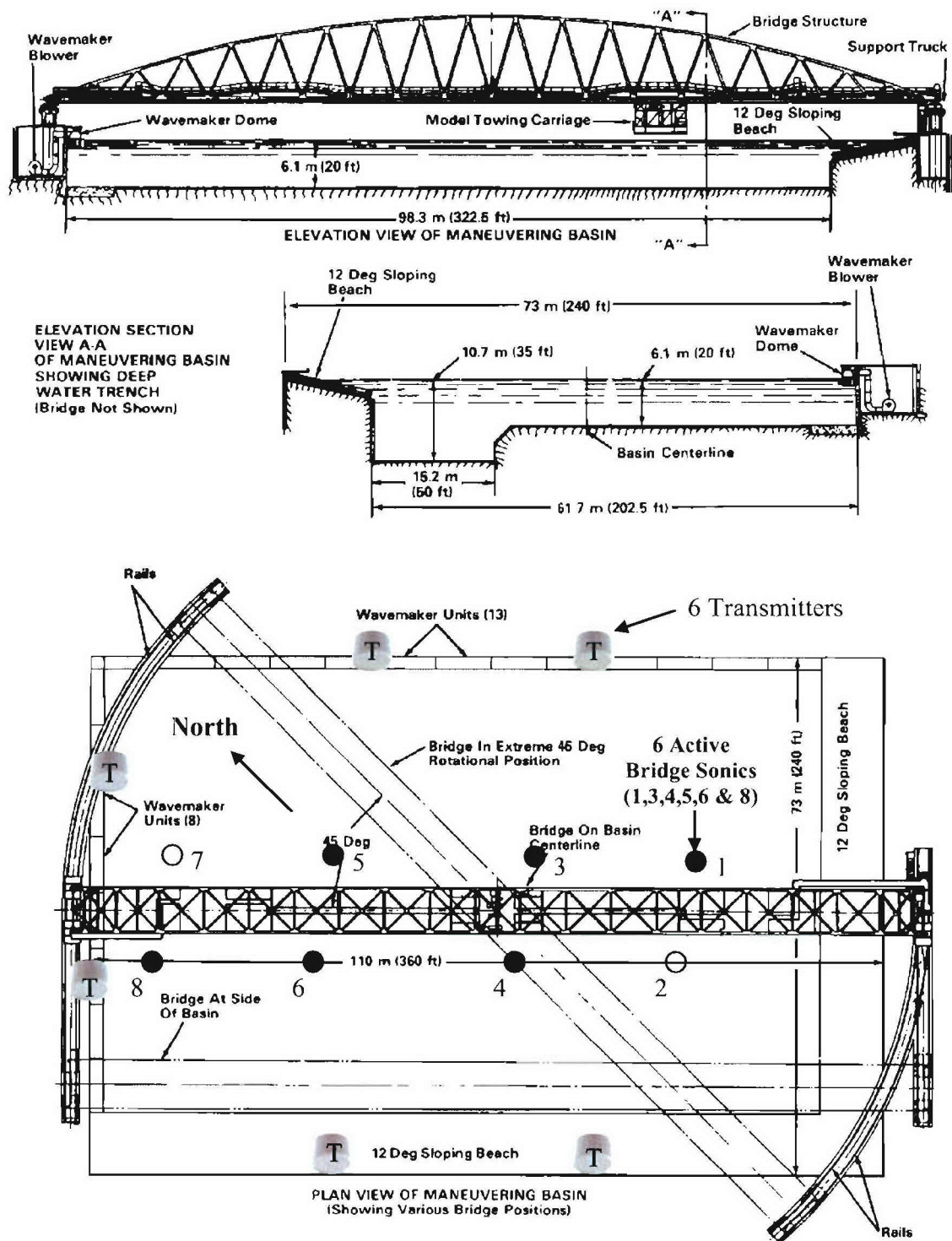


Figure 7. Sketch of Maneuvering and Seakeeping (MASK) Basin.



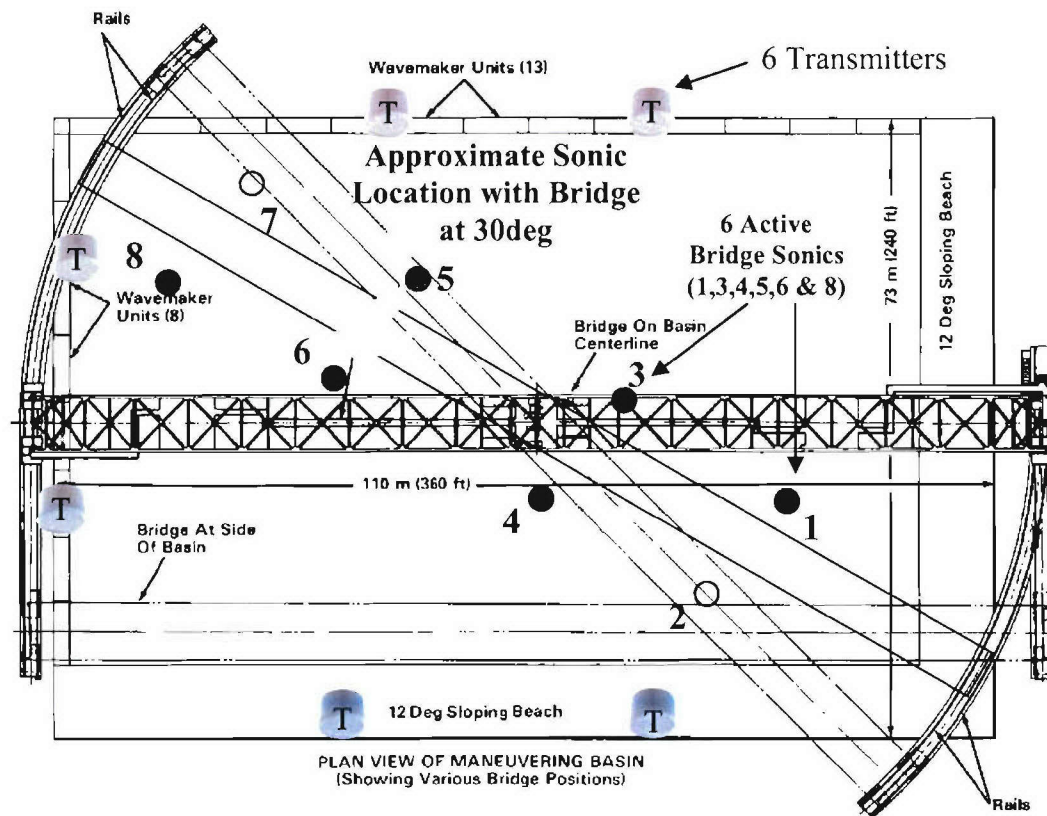
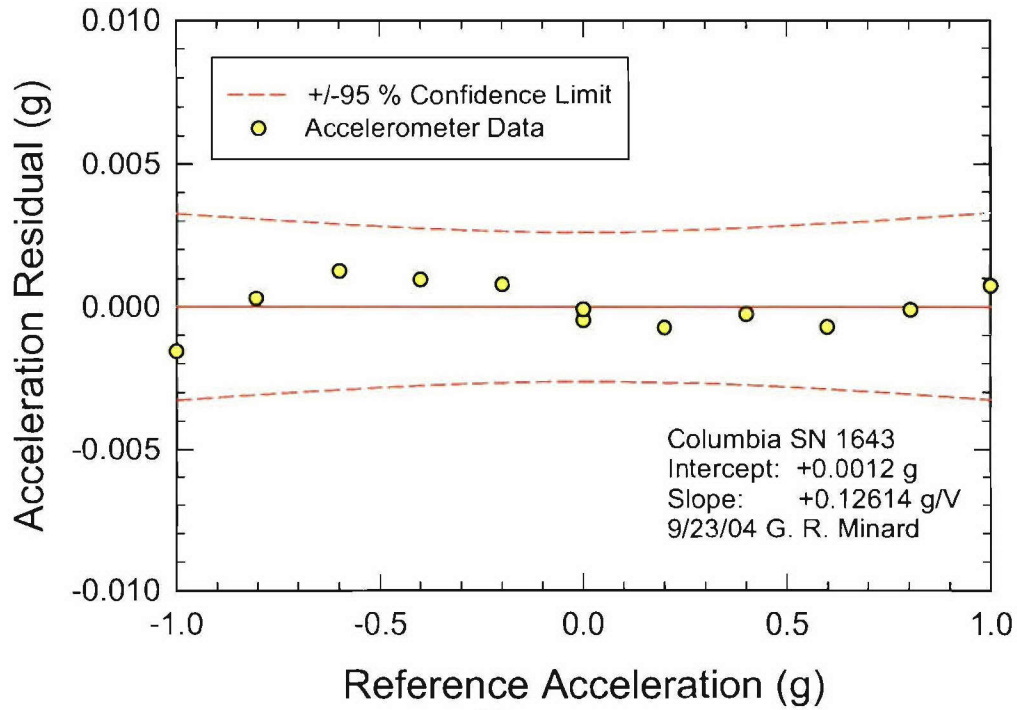
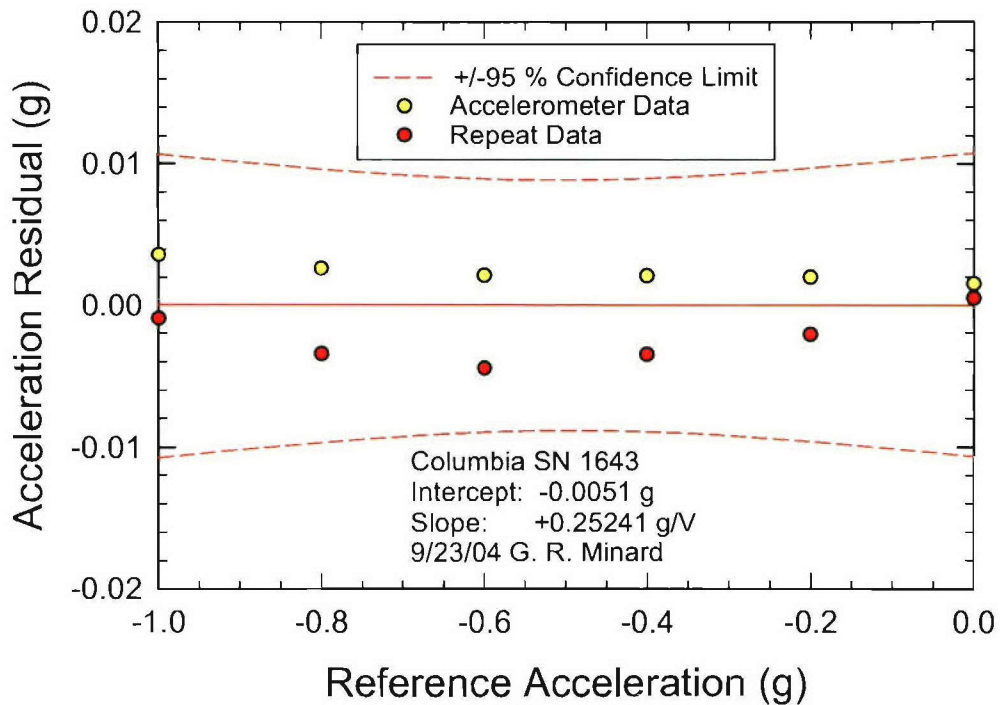


Figure 8. Relative Position of Bridge Sonics When Bridge Is At 30 Degrees.



**a. Transverse**



**b. Vertical**

Figure 9. Residuals for calibration of acceleration at CG for model 5514.

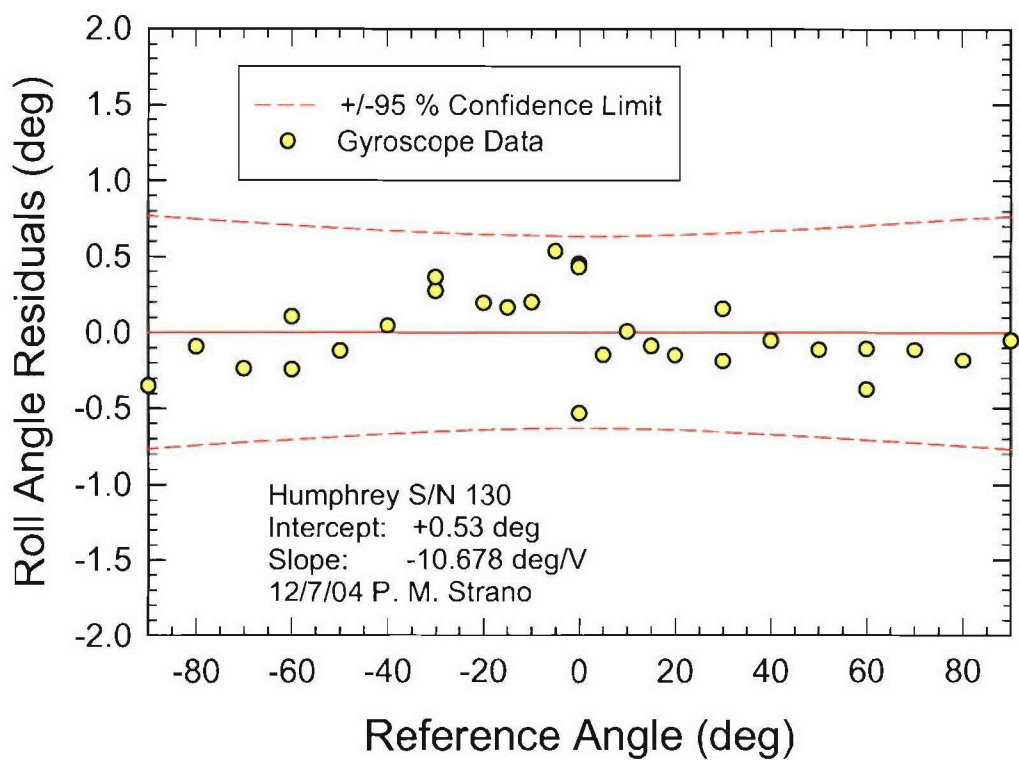


Figure 10. Residuals for calibration of roll angle for model 5514

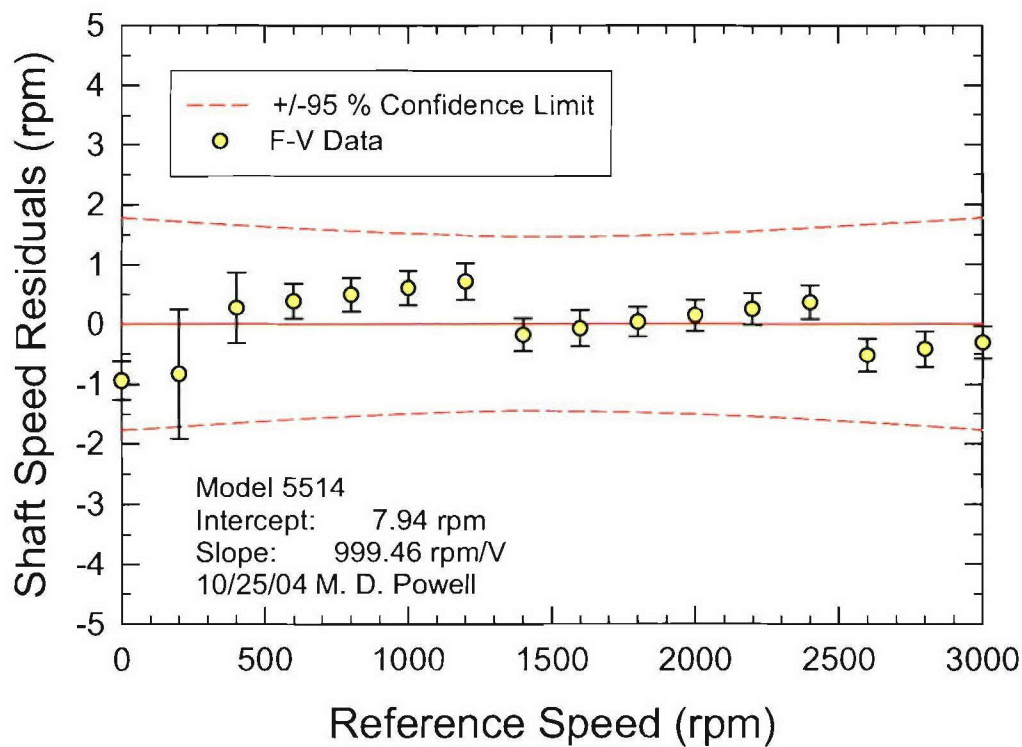


Figure 11. Residuals for calibration of propeller shaft rotational speed

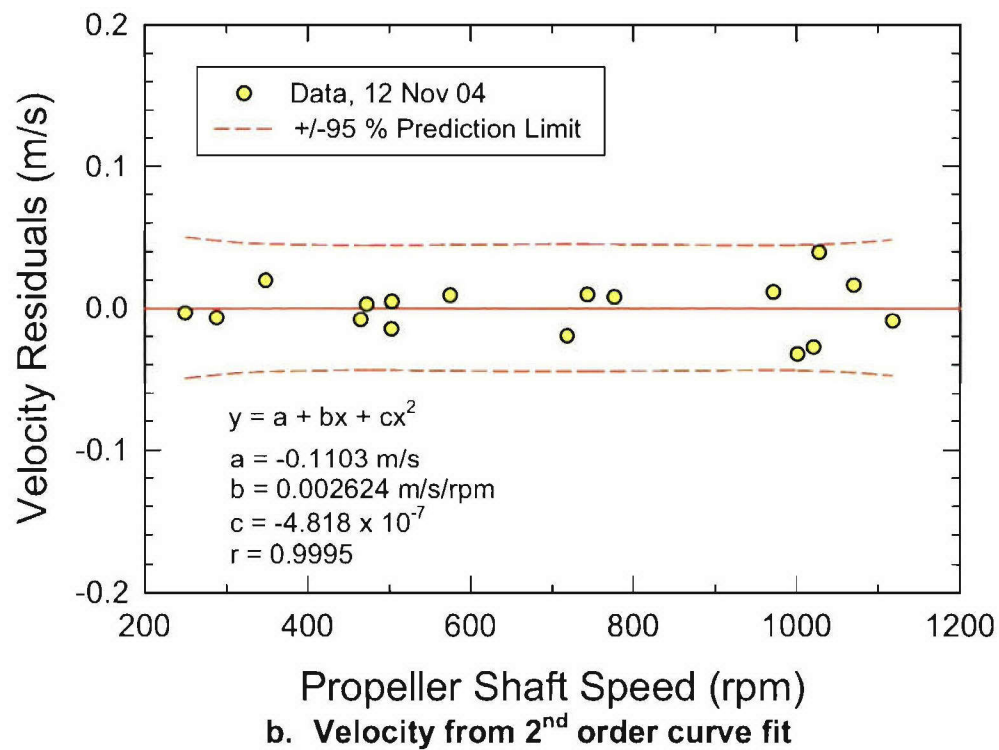
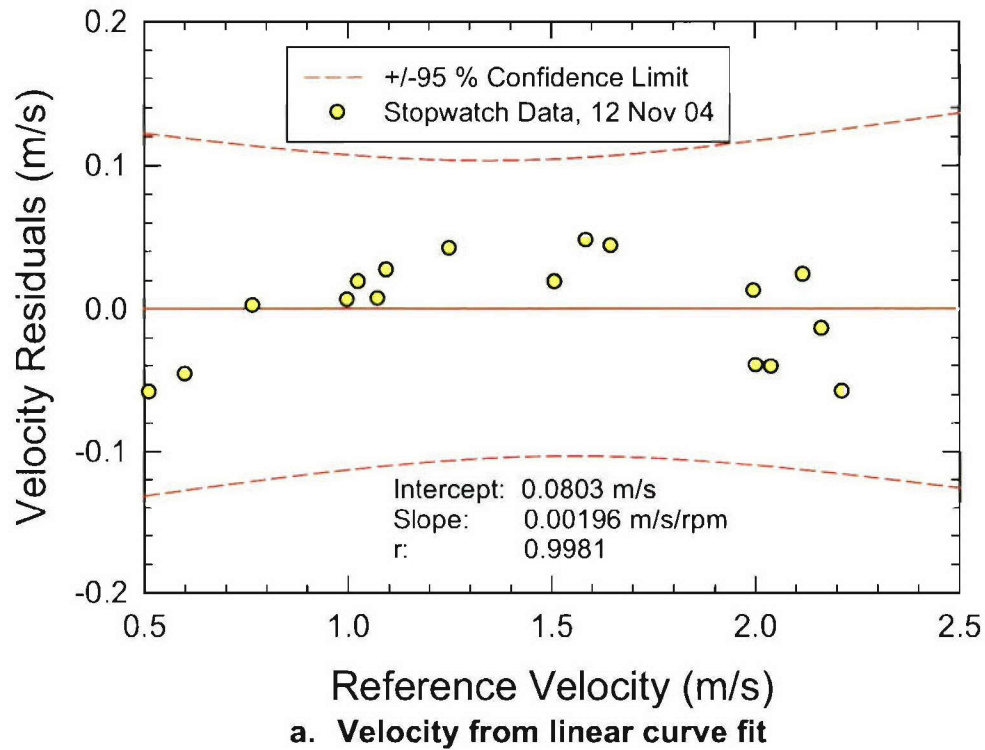


Figure 12. Residuals for calibration of model velocity for model 5514 from propeller shaft speed

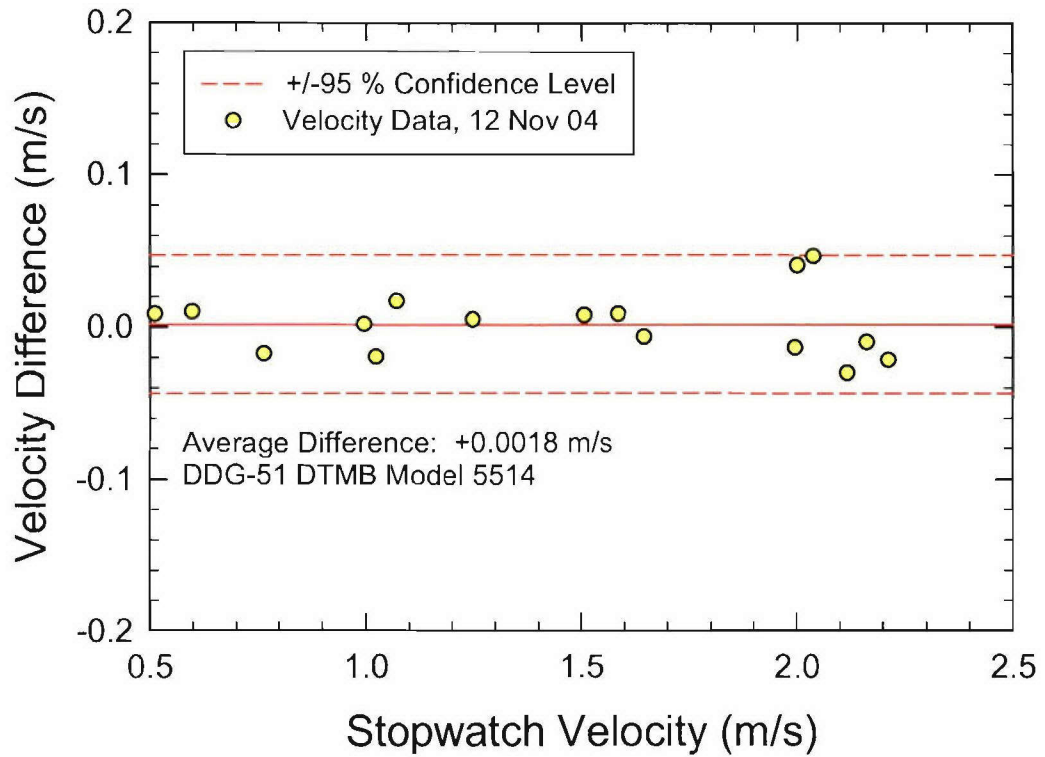


Figure 13. Comparison of model velocity from tracker to stopwatch data

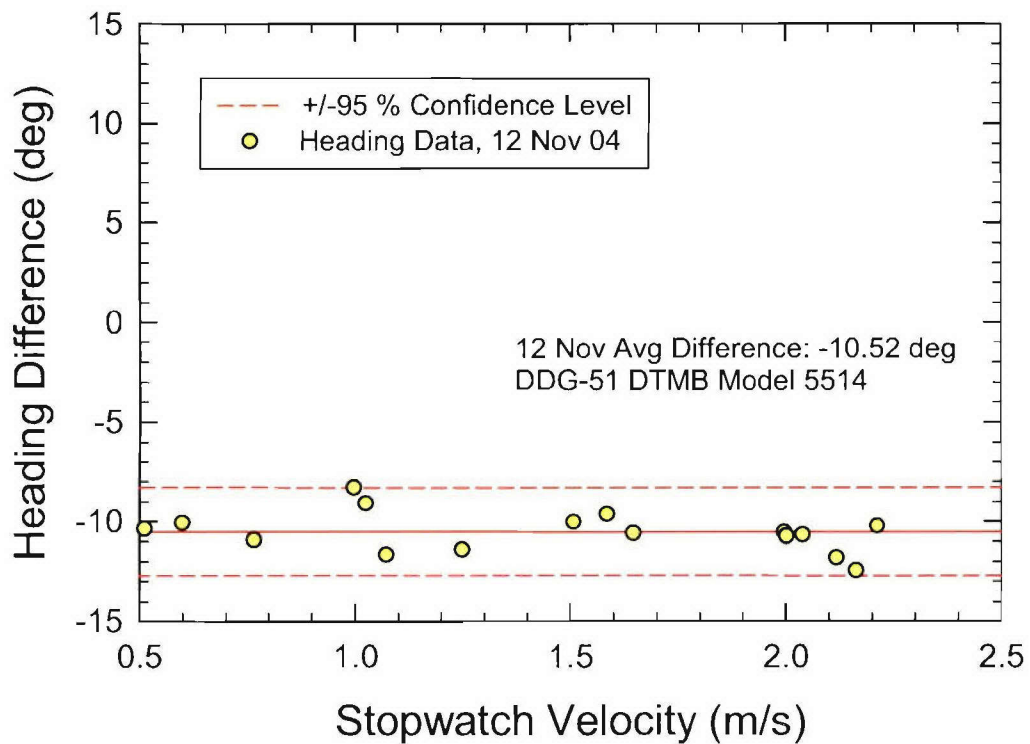


Figure 14. Comparison of tracker to model heading for model 5514



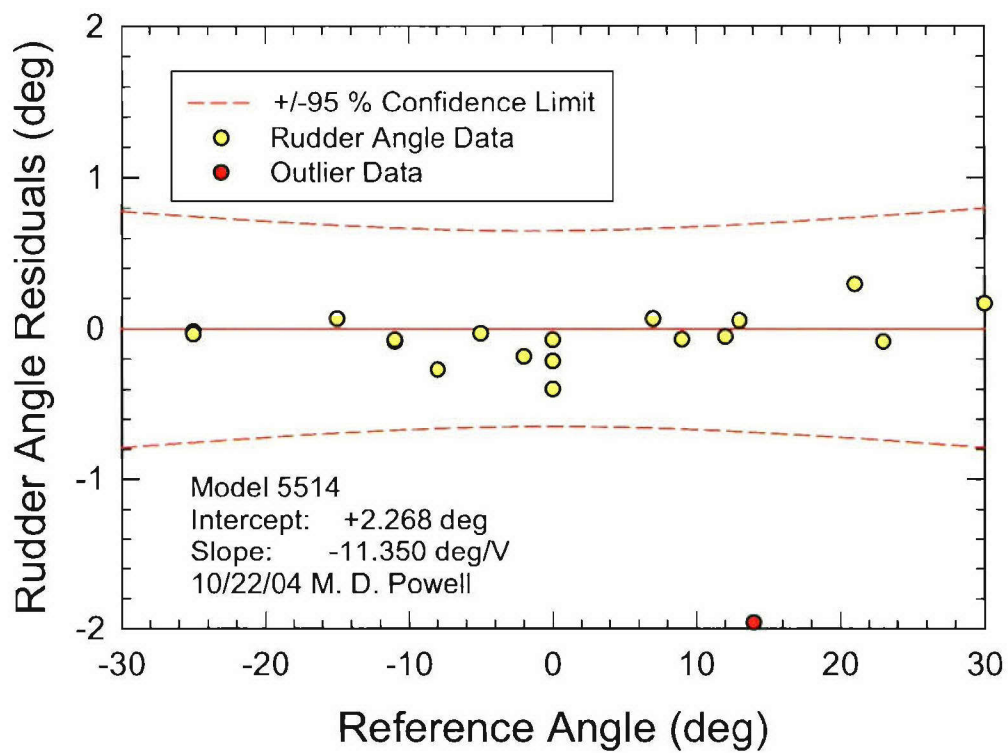


Figure 15. Residuals for calibration of rudder angle for model 5514

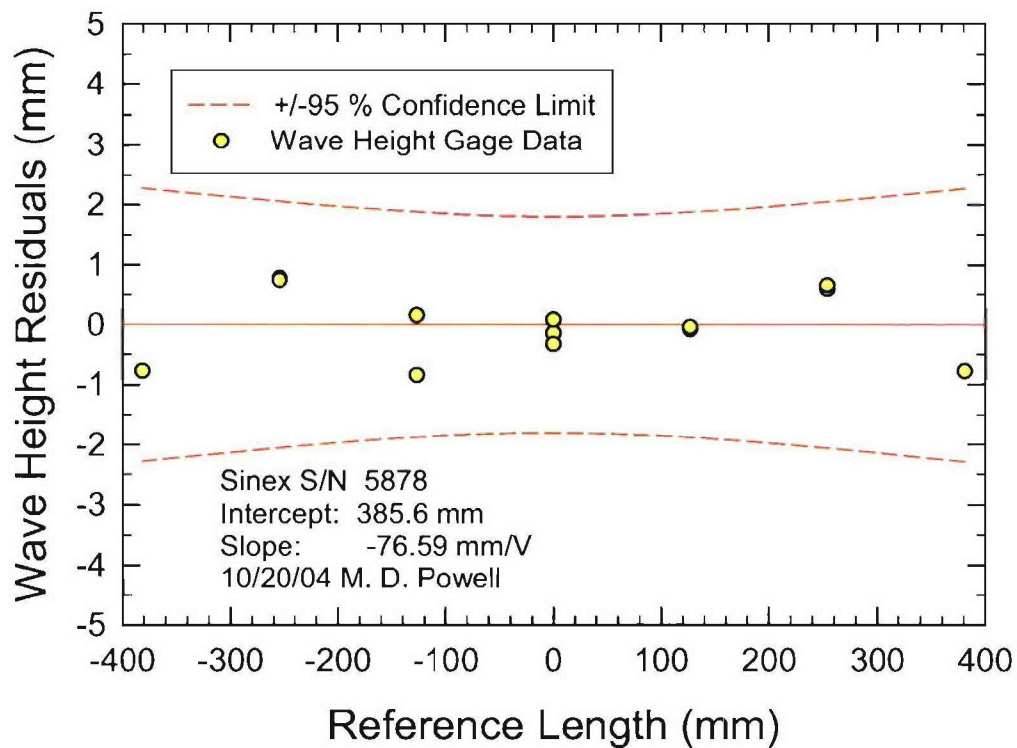


Figure 16. Residuals for calibration of Senix wave height gage #1.

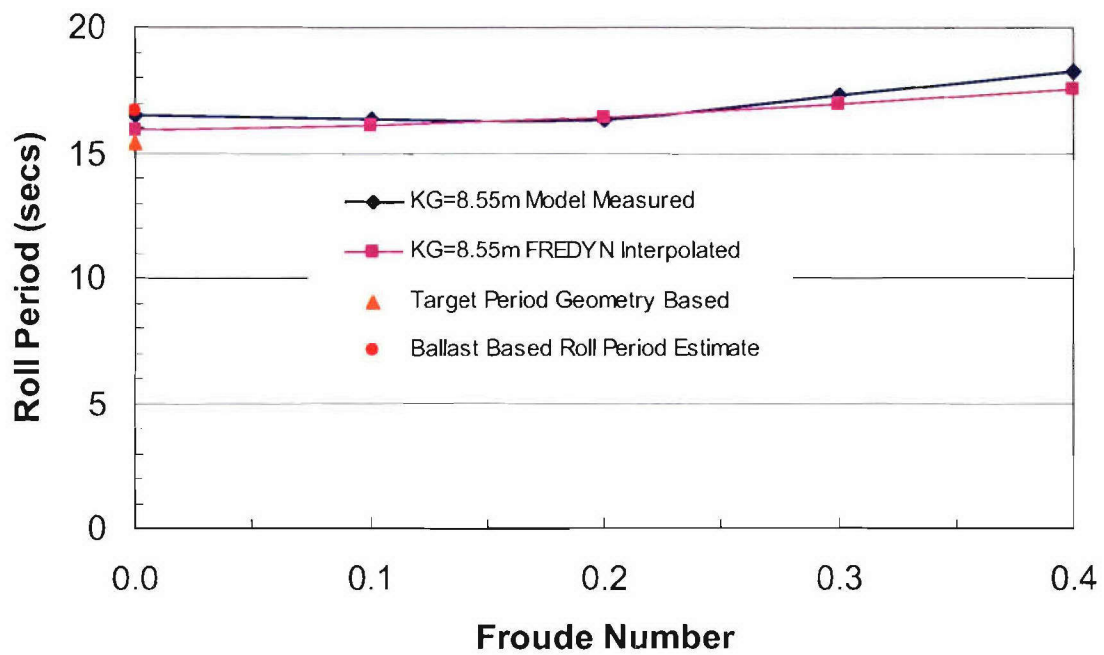


Figure 17. Roll Periods for End of Service Life, Intact 100kt Wind Limited KG.

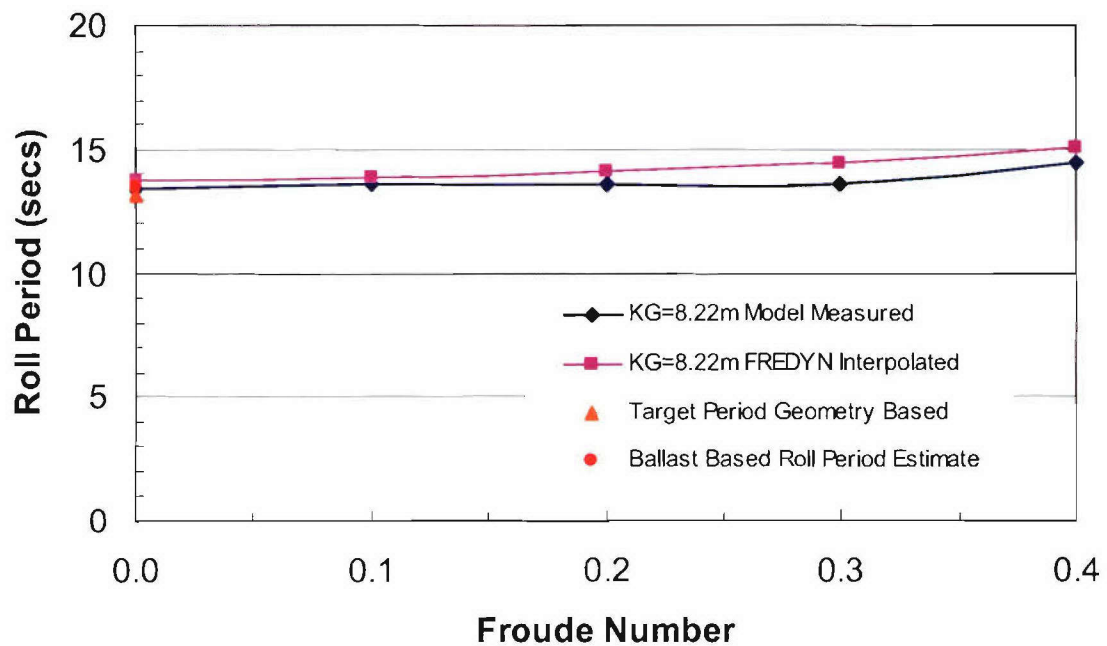


Figure 18. Roll Periods for End of Service Life, Righting Arm Limited KG.

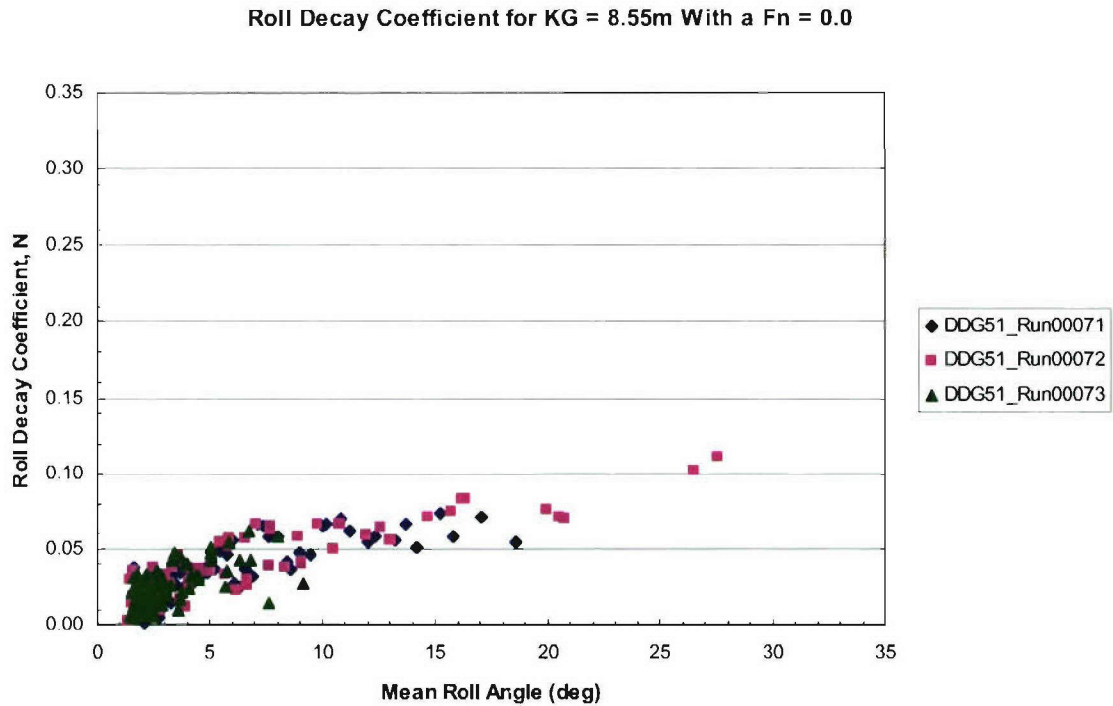


Figure 19. Roll Decay Coefficients for End of Service Life, Intact 100kt Wind Limited KG,  $F_n=0.0$ .

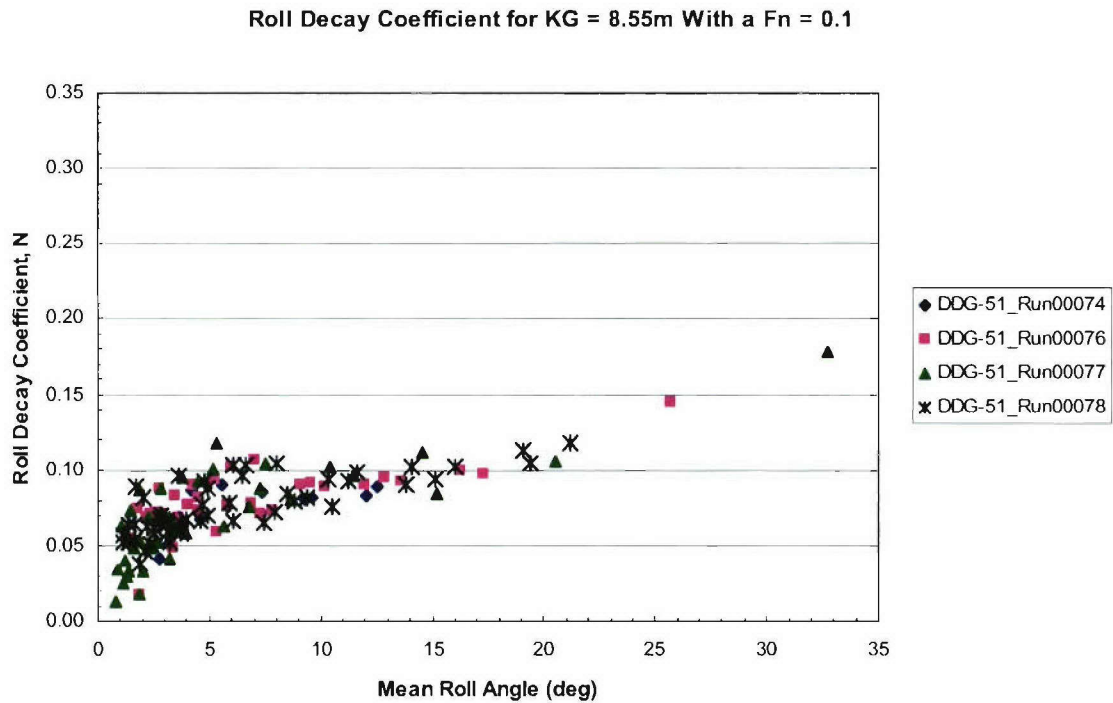


Figure 20. Roll Decay Coefficients for End of Service Life, Intact 100kt Wind Limited KG,  $F_n=0.1$ .

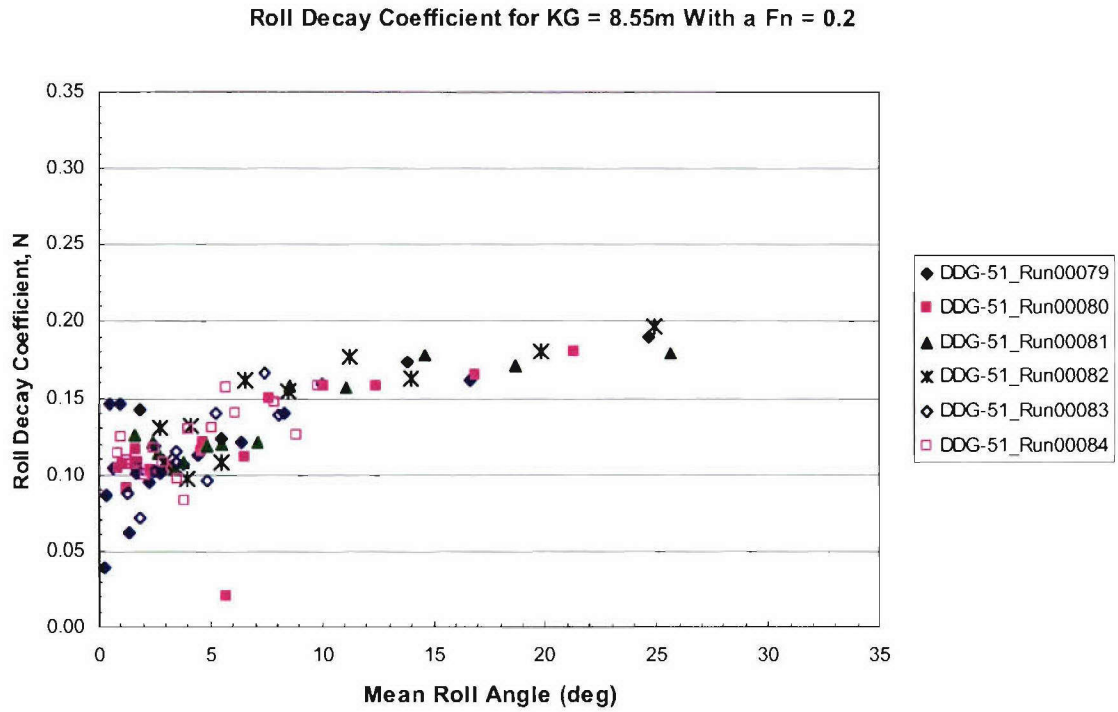


Figure 21. Roll Decay Coefficients for End of Service Life, Intact 100kt Wind Limited KG, Fn=0.2.

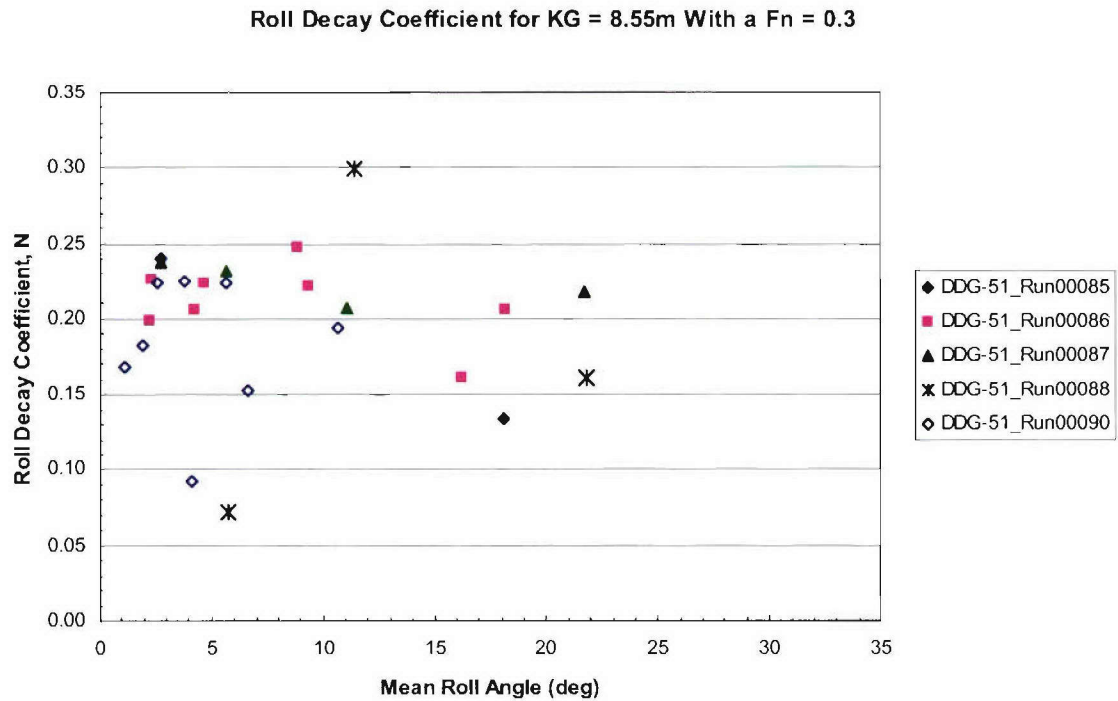


Figure 22. Roll Decay Coefficients for End of Service Life, Intact 100kt Wind Limited KG, Fn=0.3.

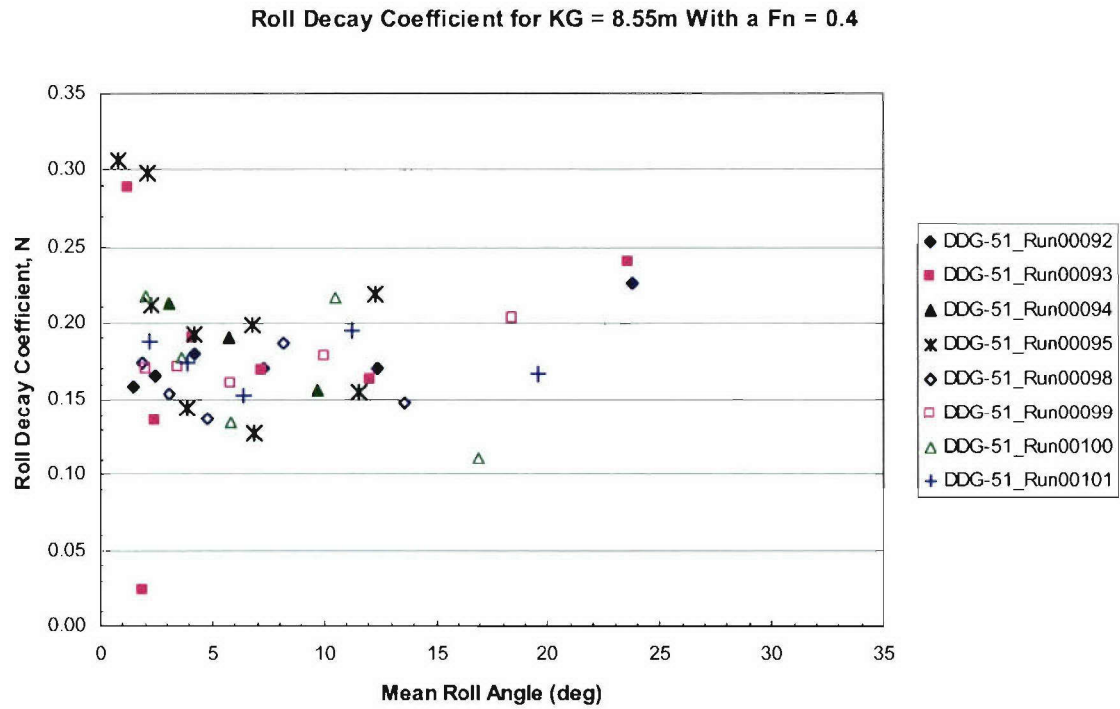


Figure 23. Roll Decay Coefficients for End of Service Life, Intact 100kt Wind Limited KG, Fn=0.4.

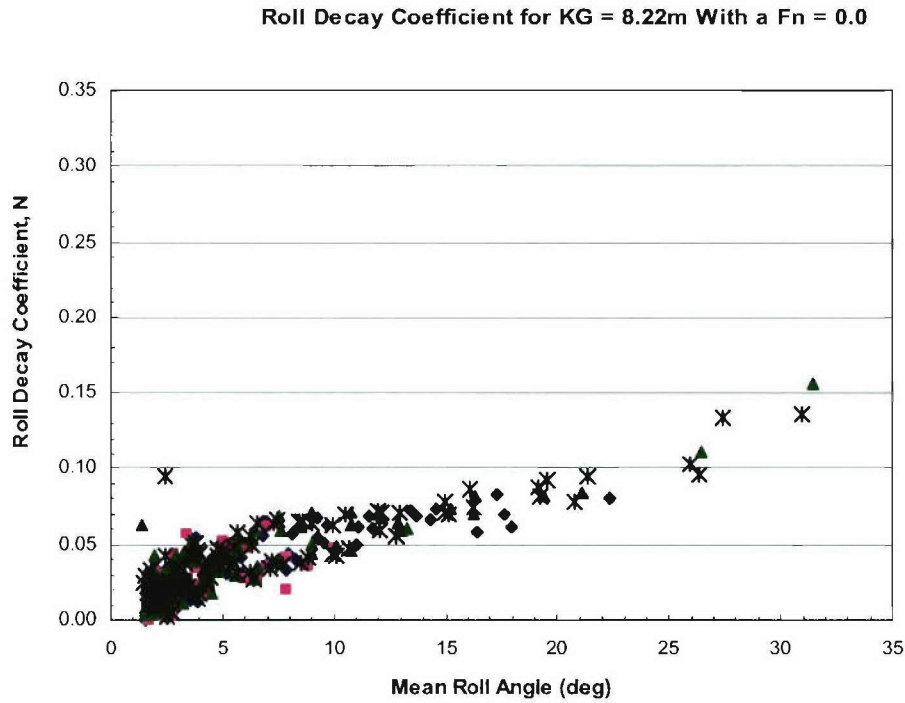


Figure 24. Roll Decay Coefficients for End of Service Life, Righting Arm Limited KG, Fn=0.0.



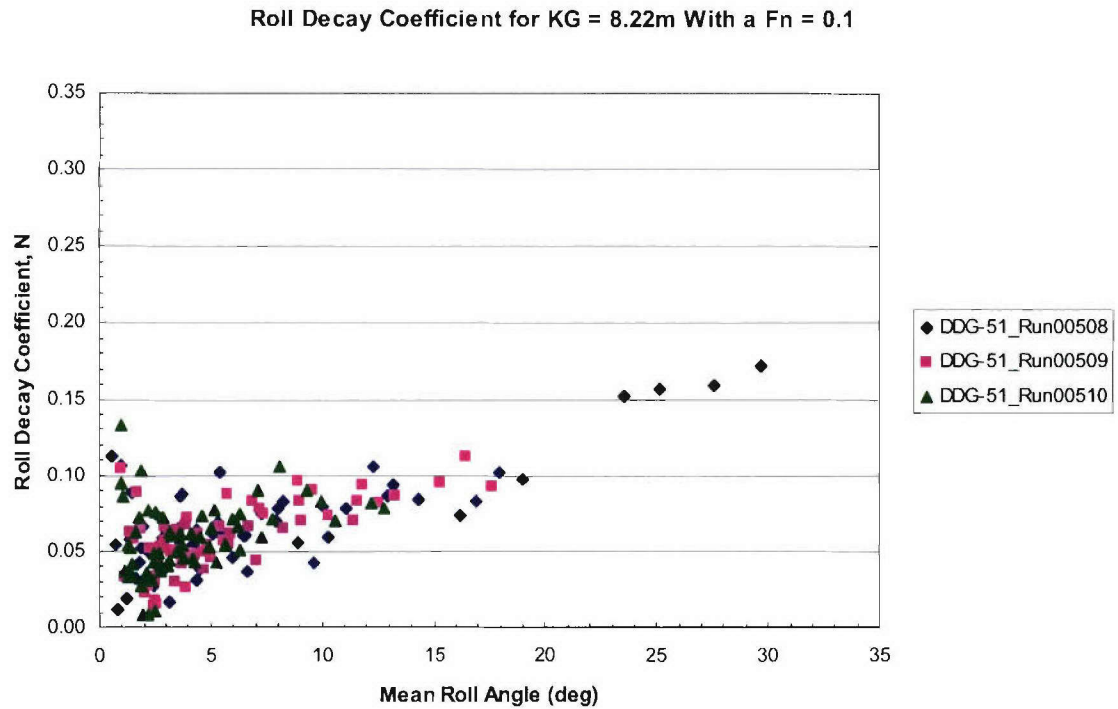


Figure 25. Roll Decay Coefficients for End of Service Life, Righting Arm Limited KG,  $F_n=0.1$ .

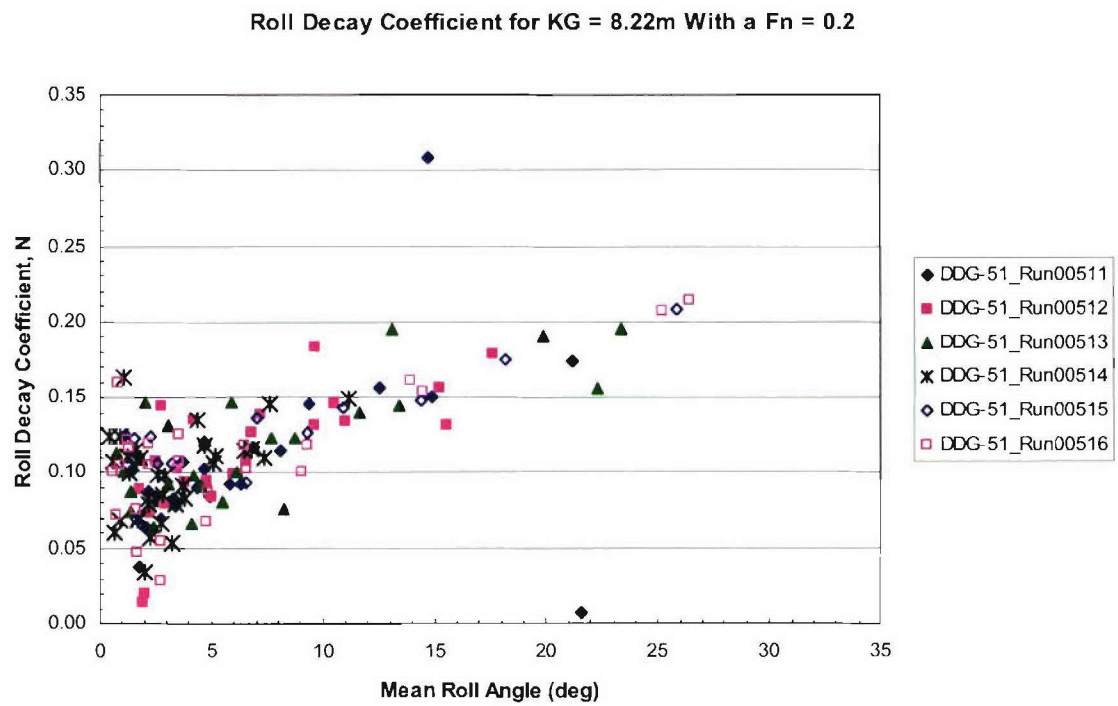


Figure 26. Roll Decay Coefficients for End of Service Life, Righting Arm Limited KG,  $F_n=0.2$ .

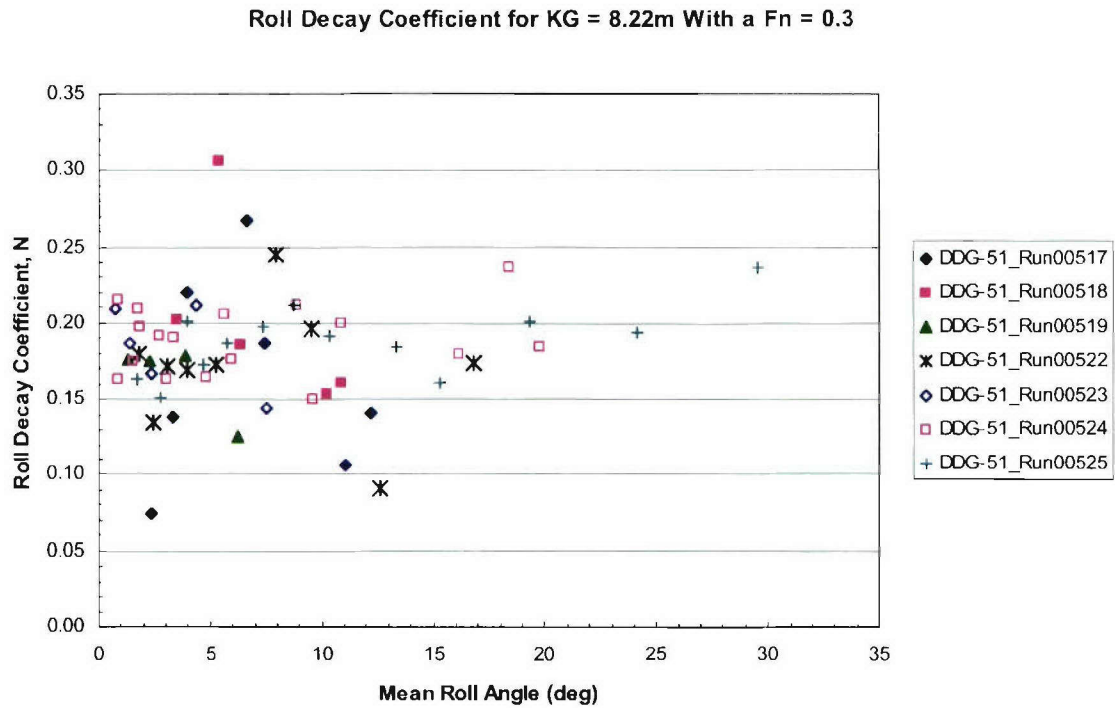


Figure 27. Roll Decay Coefficients for End of Service Life, Righting Arm Limited KG, Fn=0.3.

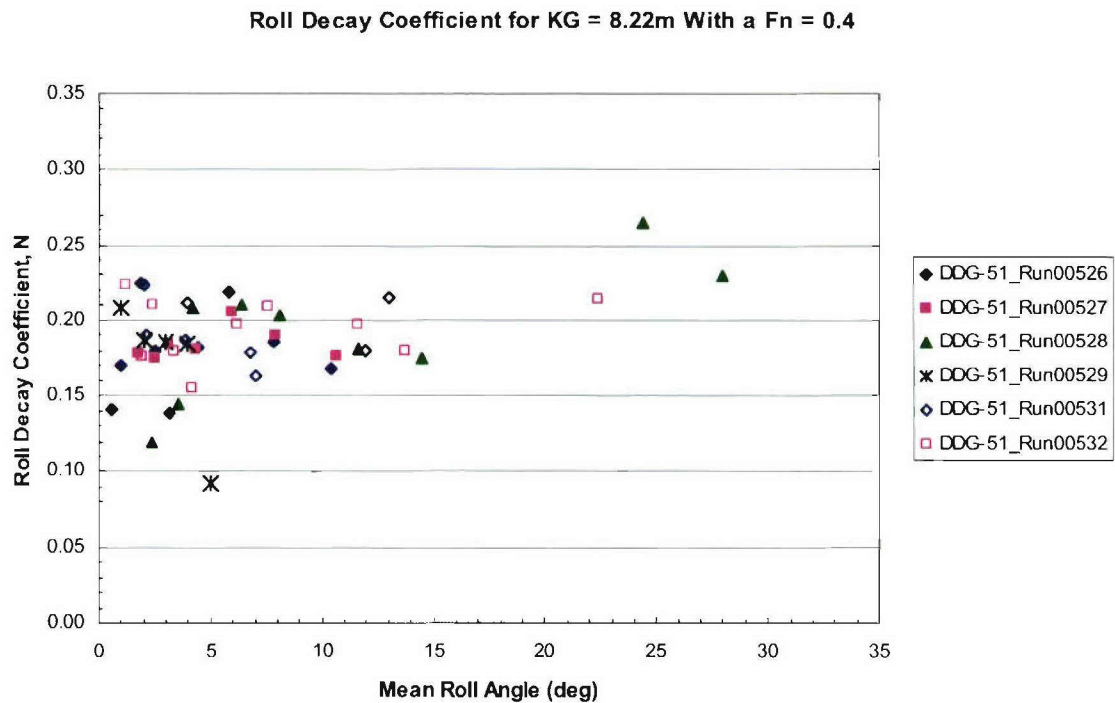


Figure 28. Roll Decay Coefficients for End of Service Life, Righting Arm Limited KG, Fn=0.4.

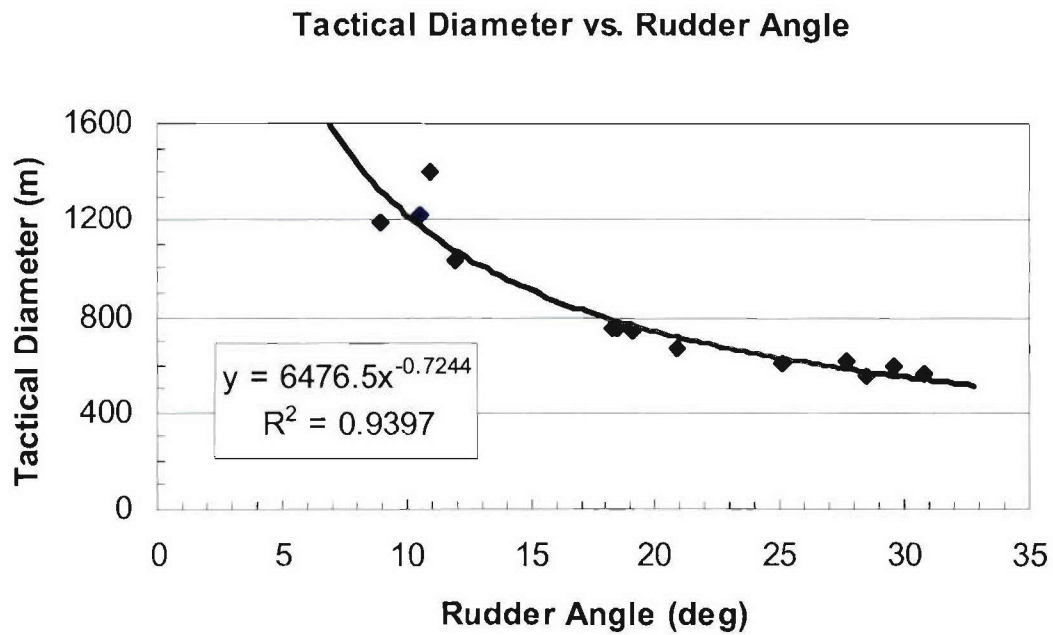


Figure 29. Plot and Curve Fit of Tactical Diameter Versus Rudder Angle for all Speeds.

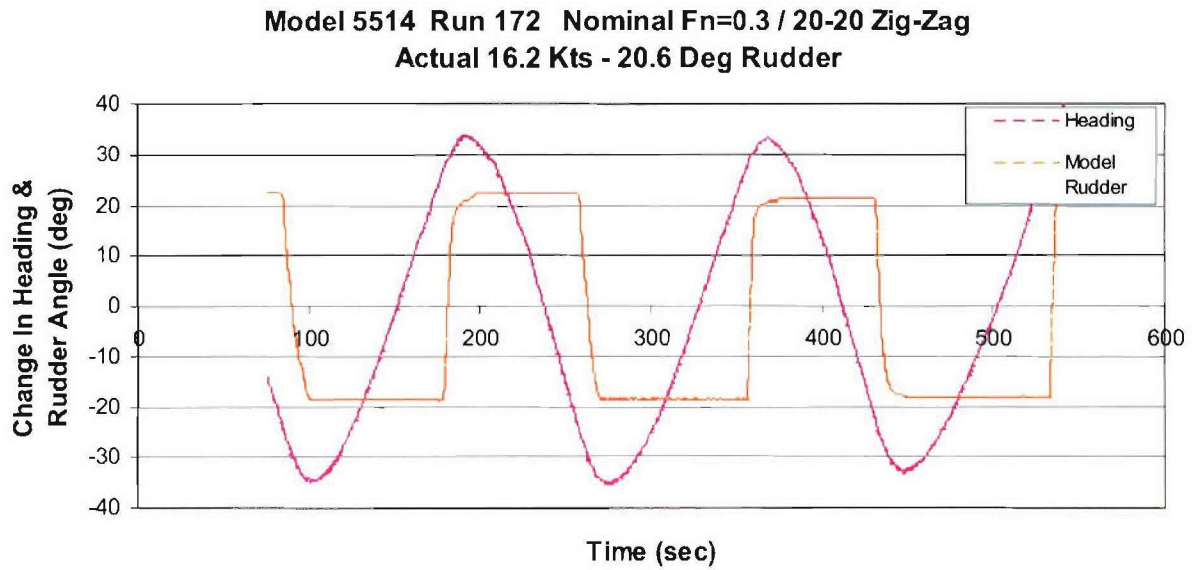


Figure 30. Example Zig-Zag Maneuver – Run 172.

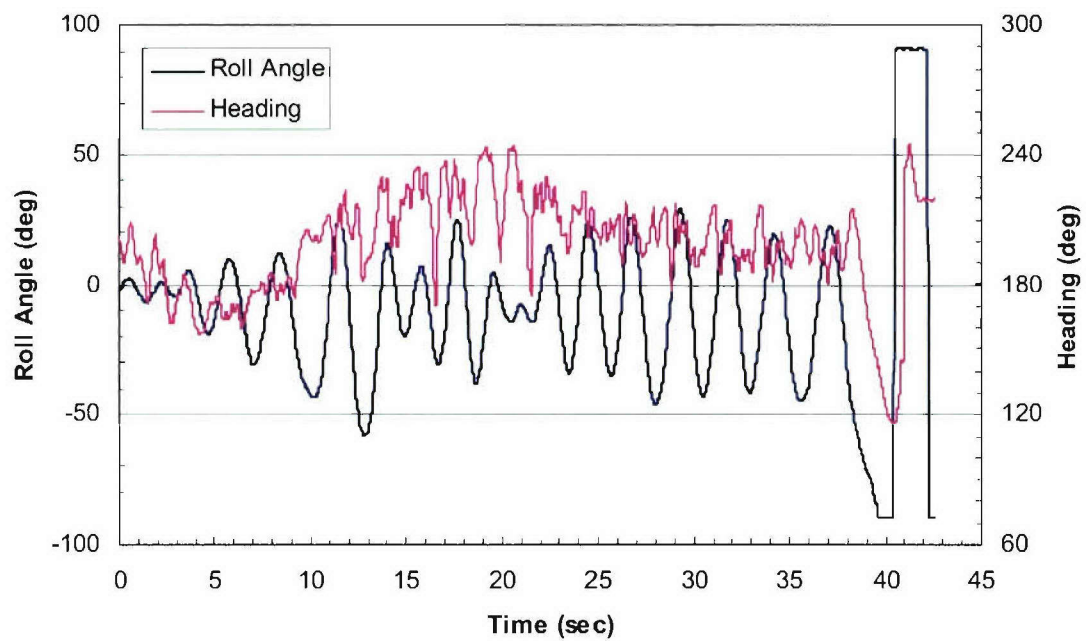
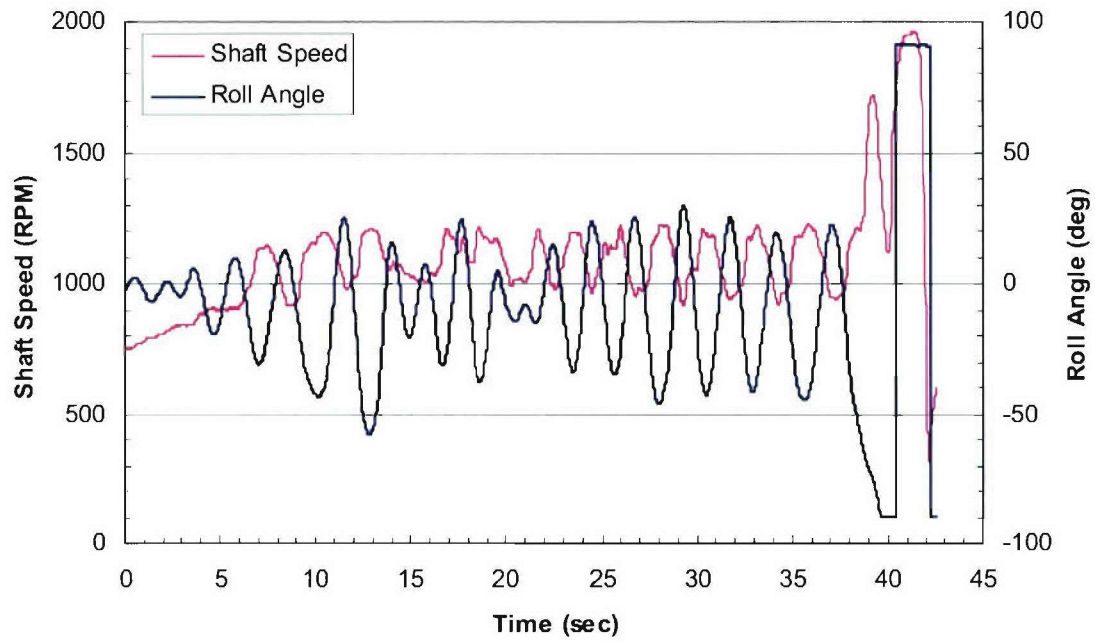


Figure 31. Time Histories Reviewed to Assure Quality of Capsize Condition – Run 411.

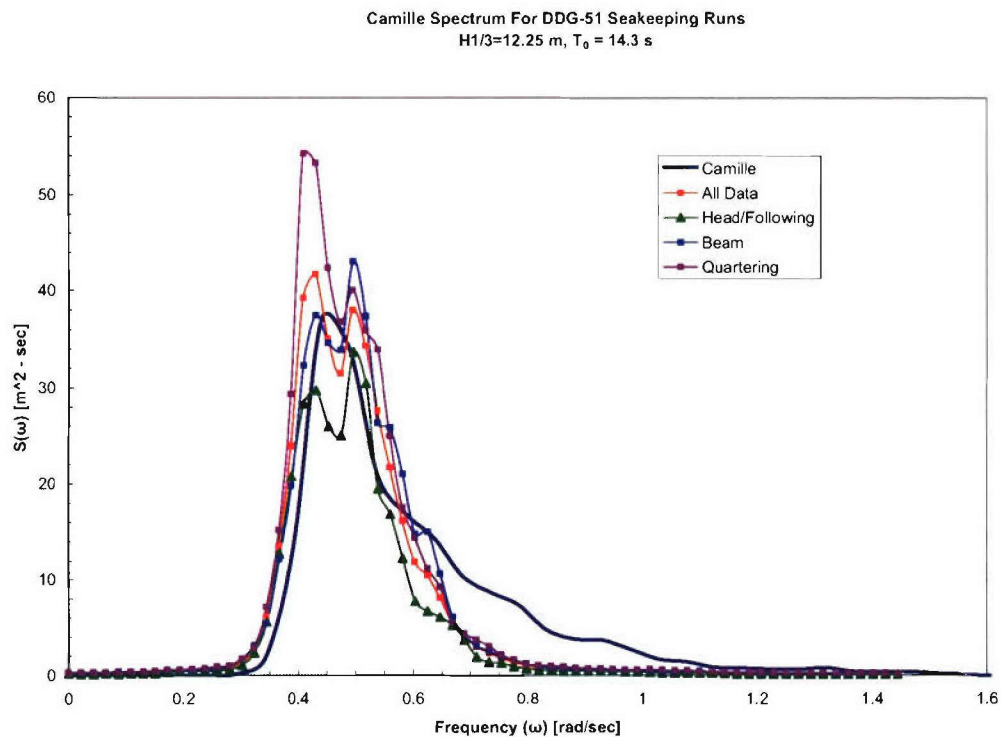


Figure 32. Wave Spectra collected during Hurricane Camille Runs.

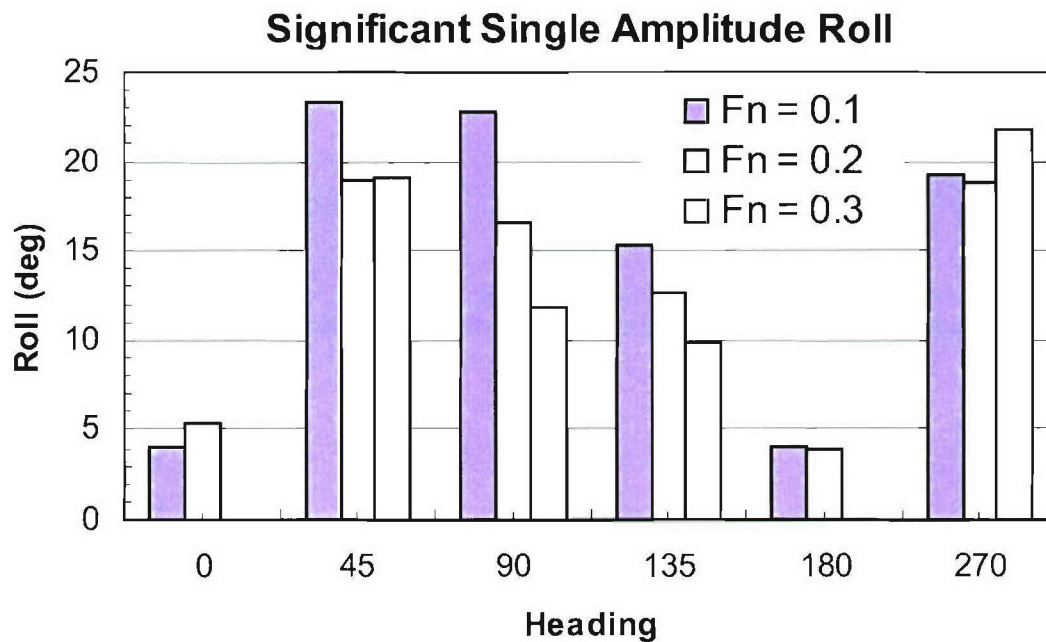


Figure 33. Plot of Significant Single Amplitude Roll in Sea State 8 – Hurricane Camille.



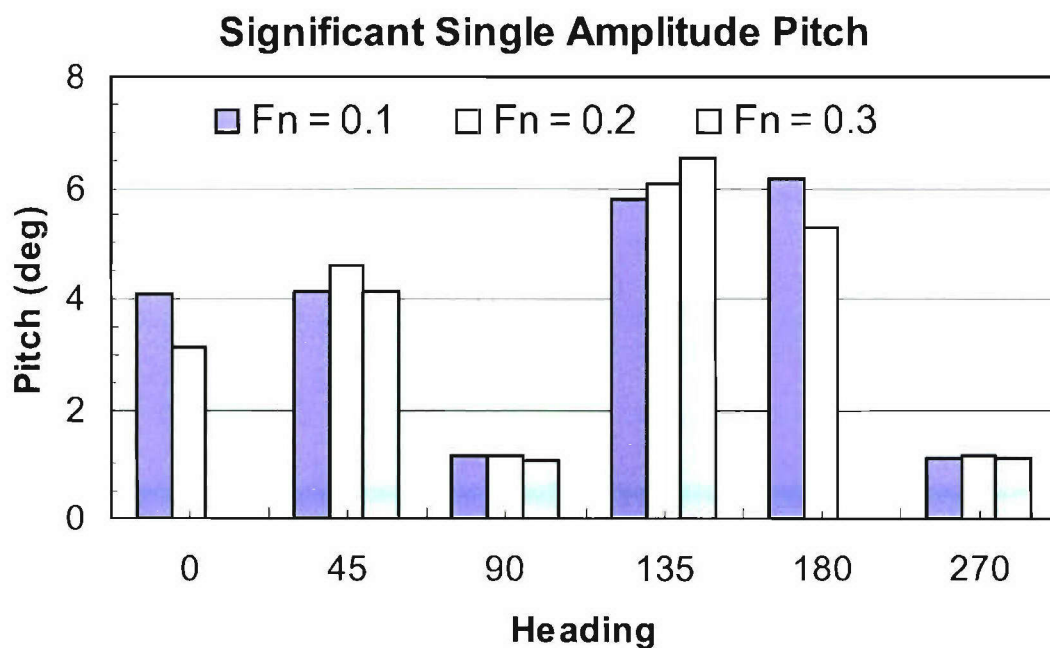


Figure 34. Plot of Significant Single Amplitude Pitch in Sea State 8 – Hurricane Camille.

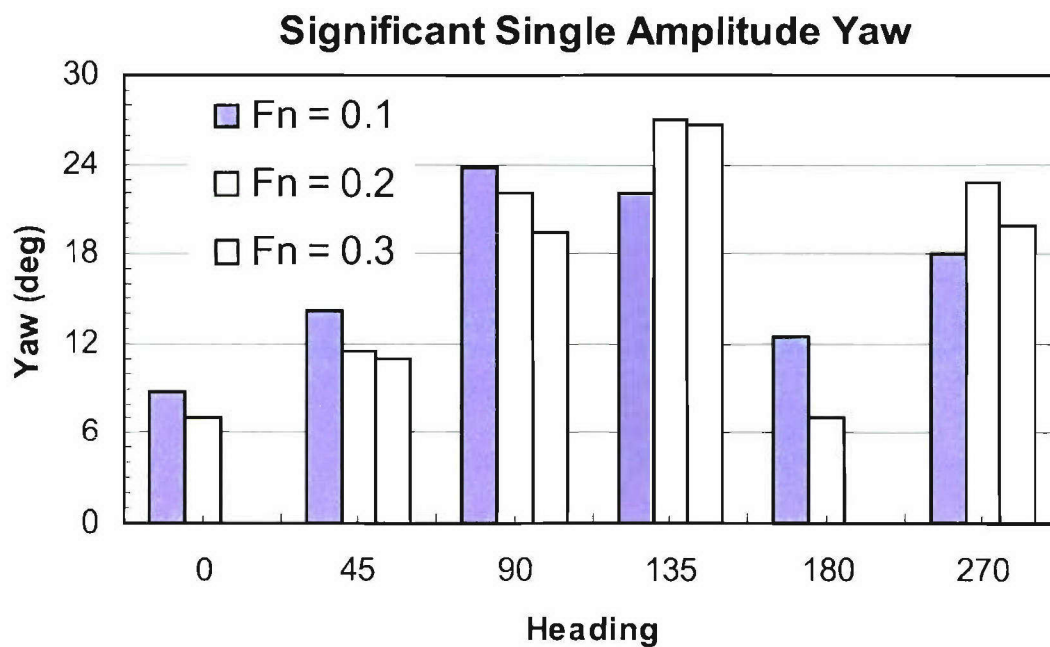


Figure 35. Plot of Significant Single Amplitude Yaw in Sea State 8 – Hurricane Camille.

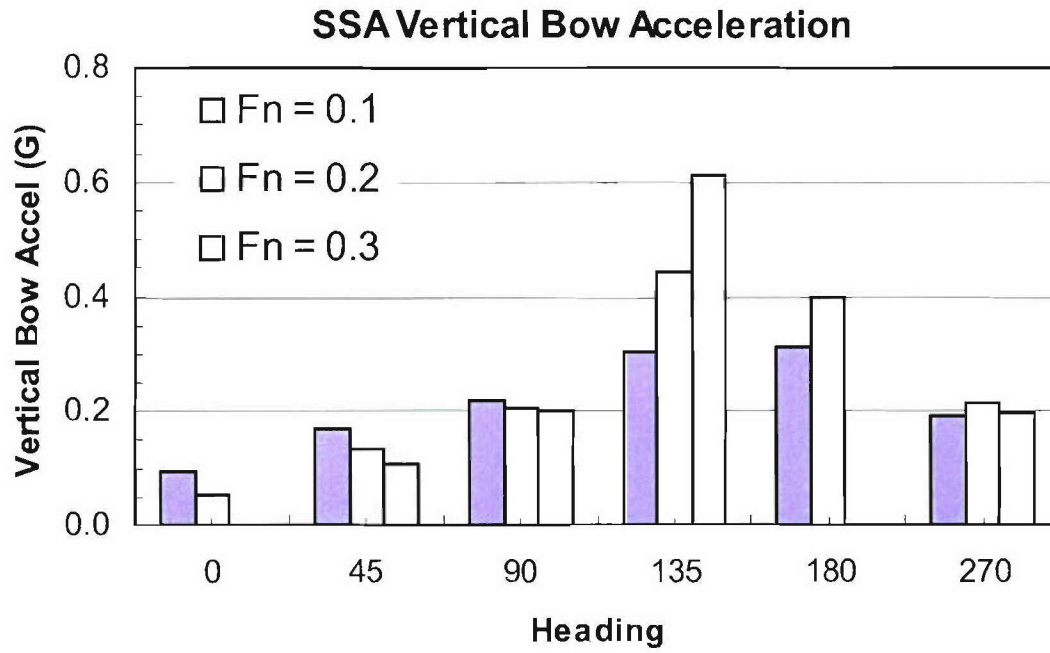


Figure 36. Plot of SSA Vertical Bow Acceleration in Sea State 8 – Hurricane Camille.

Table 1. Comparison of Pre-Contract DDG51 as Compared to As-Built DDG51 and DDG79.

	DDG51 Pre-Contract				DDG51 As Built				DDG51 Flight Deck IIA As Built			
	English		Metric		English		Metric		English		Metric	
LOA	481.00	ft	146.61	m	498.04	ft	151.80	m	509.50	ft	155.30	m
LBP		ft		m	466.00	ft	142.04	m	471.00	ft	143.56	m
LWL	466.00	ft	142.04	m	466.03	ft	142.05	m	471.00	ft	143.56	m
Beam (WL)	62.90	ft	19.17	m	59.19	ft	18.04	m	59.00	ft	17.98	m
<b>End of Service Life</b>												
Draft	21.37	ft SW	6.51	m	22.25	ft SW	6.78	m	23.02	ft SW	7.02	m
Trim	0.36	ft	0.11	m	0.00	ft	0.00	m	0.29	ft	0.09	m
Displacement	9400.00	l-tons SW	9549.21	m-ton	9500.00	l-tons SW	9652.45	m-ton	9987.00	l-tons SW	10147.26	m-ton
Depth	41.83	ft	12.75	m		ft	0.00	m	41.83	ft	12.75	m
LCG	-5.90	ft	-1.80	m	-2.21	ft	-0.67	m	-3.86	ft	-1.18	m
VCG	28.06	ft	8.55	m	25.27	ft	7.70	m	25.71	ft	7.84	m
KM	31.06	ft	9.47	m	29.01	ft	8.84	m	29.09	ft	8.87	m
GM	3.00	ft	0.91	m	3.74	ft	1.14	m	3.38	ft	1.03	m

Table 2. General Conditions Performed for Model 5514, Pre-Contract DDG51 Capsize Test.

Loading Condition and KG/GM Definition	Test Type	
	Regular Wave Dynamic Stability	Storm Spectra - Hurricane Camille
End of Service Life / Intact 100 kt Wind Limiting KG	Runs 193 - 446	Condition Not Tested
End of Service Life / Righting Arm Limiting KG	Runs 550 - 598	Runs 601 - 659

Table 3. Mass Properties End of Service Life Load Limit, Intact 100 kt Wind Limiting KG.

	FULL SCALE		MODEL SCALE DESIRED		MODEL SCALE ACHIEVED	
	Values English	Values Metric	Values English	Values Metric	Values English	Values Metric
<b>Displacement</b>	9400.00 LSW	9549.21 m-ton SW	202.87 lbs FW	92.10 kg FW	202.46 lbs FW	91.92 kg FW
<b>LCG wrt Station 10</b>	-5.90 ft	-1.80 m	-1.52 in	-3.86 cm	-1.52 in	-3.86 cm
<b>KG</b>	28.06 ft	8.55 m	7.23 in	18.35 cm	7.12 in	18.08 cm
<b>Draft</b>	21.37 ft	6.51 m	5.50 in	13.98 cm	NA	NA
<b>Trim</b>	0.36 ft	0.11 m	0.09 in	0.24 cm	NA	NA
<b>GM<sub>w/FS</sub></b>	3.00 ft	0.91 m	0.77 in	1.96 cm	0.76 in	1.93 cm
<b>k<sub>pitch</sub></b>	116.50 ft	35.51 m	30.00 in	76.20 cm	29.73	75.52 cm
<b>k<sub>pitch</sub>/LBP</b>	0.250	0.250	0.250	0.250	0.248	0.248
<b>k<sub>roll</sub></b>	24.09 ft	7.34 m	6.20 in	15.76 cm	6.67	16.94 cm
<b>k<sub>roll</sub>/Beam<sub>WL</sub></b>	0.383	0.383	0.383	0.383	0.412	0.412
<b>Roll Period<sub>Zero Speed</sub></b>	15.41	15.41	2.257	2.257	2.421 sec	2.421 sec

Table 4. Mass Properties End of Service Life Load Limit, Righting Arm Limiting KG.

	FULL SCALE		MODEL SCALE DESIRED		MODEL SCALE ACHIEVED	
	Values English	Values Metric	Values English	Values Metric	Values English	Values Metric
<b>Displacement</b>	9400.00 LSW	9550.85 m-ton SW	202.87 lbs FW	92.10 kg FW	202.46 lbs FW	91.92 kg FW
<b>LCG wrt Station 10</b>	-5.90 ft	-1.80 m	-1.52 in	-3.86 cm	-1.52 in	-3.86 cm
<b>KG</b>	26.97 ft	8.22 m	6.95 in	17.64 cm	6.81 in	17.29 cm
<b>Draft</b>	21.37 ft	6.51 m	5.50 in	13.98 cm	NA	NA
<b>Trim</b>	0.36 ft	0.11 m	0.09 in	0.24 cm	NA	NA
<b>GM<sub>w/FS</sub></b>	4.09 ft	1.25 m	1.05 in	2.68 cm	1.04 in	2.63 cm
<b>k<sub>pitch</sub></b>	116.50 ft	35.51 m	30.00 in	76.20 cm	29.65	75.31 cm
<b>k<sub>pitch</sub>/LBP</b>	0.250	0.250	0.250	0.250	0.247	0.247
<b>k<sub>roll</sub></b>	24.09 ft	7.34 m	6.20 in	15.76 cm	6.29	15.97 cm
<b>k<sub>roll</sub>/Beam<sub>WL</sub></b>	0.383	0.383	0.383	0.383	0.388	0.388
<b>Roll Period<sub>Zero Speed</sub></b>	13.19	13.19	1.933	1.933	1.971 sec	1.971 sec

Table 5. Rudder and Propeller Characteristics for Model 5514.

	FULL SCALE		MODEL SCALE DESIRED		MODEL SCALE ACHIEVED	
	Values English	Values Metric	Values English	Values Metric	Values English	Values Metric
<b>Propeller Type</b>	Controllable Pitch		Controllable Pitch		Fixed	
<b>Number of Blades</b>	5		5		4	
<b>Diameter</b>	17.00 ft	5.18 m	4.38 in	9.39 cm	5.00 in	10.73 cm
<b>Pitch at 0.7 Radius</b>	29.20 ft	8.90 m	7.52 in	16.14 cm	7.00 in	15.02 cm
<b>Expanded Area Ratio</b>	0.79		0.79			
<b>Root Chord</b>	14.90 ft	4.54 m	3.84 in	8.23 cm	3.57 in	7.65 cm
<b>Tip Chord</b>	7.88 ft	2.40 m	2.03 in	4.35 cm	1.61 in	3.45 cm
<b>Span</b>	13.42 ft	4.09 m	3.45 in	7.41 cm	3.90 in	8.37 cm
<b>CL Stock to Root LE</b>	4.46 ft	1.36 m	1.15 in	2.46 cm	1.07 in	2.30 cm
<b>CL Stock to Tip LE</b>	0.75 ft	0.23 m	0.19 in	0.41 cm	0.11 in	0.24 cm
<b>Rudder Lateral Area</b>	152.78 ft <sup>2</sup>	14.19 m <sup>2</sup>	10.13 in <sup>2</sup>	46.65 cm <sup>2</sup>	10.09 in <sup>2</sup>	46.45 cm <sup>2</sup>

Table 6. List of Model Data Channels and Calibrations for Model 5514.

Channel Name	Units	Source	Cal Factor	Intercept	Manufacturer	Type Transducer	Model	Serial Number	Long Location (MS in)	Tran Location (MS in)	Vertical Location (MS in)
Shaft Speed	RPM	Sensor	999.4600	7 9370	Pepperl+Fuchs / Analog Devices / NSWCCD	Optical Pulser / F to V / Electronic Circuit	OBS2000-F28-E4 / 451J / NA	NA	-20.00	3.63	7.15
Rudder	Deg	Sensor	-11.3485	2.2674	Bourns	Rotary Potentiometer	6574S-1-103	NA	-32.31	-2.94	8.33
KVH Sin	volts	Sensor	1.0000	0.0000	KVH	Fluxgate Compass	C-100	NA	7.08	0.00	0.00
KVH Cos	volts	Sensor	1.0000	0.0000							
KVH Ref	volts	Sensor	1.0000	0.0000							
Roll Angle	Deg	Sensor	-10.7493	-0.1892	BF Goodrich	Vertical Gyro	VG34-0809-1	130	-1.52	-5.75	7.49
Pitch Angle	Deg	Sensor	7.1290	0.2800							
Roll Rate	Deg/s	Sensor	20.0000	0.0000	BEI Systron Donner	Angular Rate Sensor	QRS14-00100-103	39522	4.49	3.26	8.39
Pitch Rate	Deg/s	Sensor	20.0000	0.0000	BEI Systron Donner	Angular Rate Sensor	QRS14-00100-103	39415	6.35	4.69	8.52
Yaw Rate	Deg/s	Sensor	10.0000	0.0000	BEI Systron Donner	Angular Rate Sensor	QRS14-00050-103	39527	4.61	5.18	7.08
Vert CG Accel	G	Sensor	0.2524	-0.0051	Columbia	Tri-Axial Mass Accelerometer	SA307TX	1643	-1.52	0.00	7.49
Trans CG Accel	G	Sensor	0.1261	0.0012							
Long CG Accel	G	Sensor	0.1262	0.0003							
Vert Bow Accel	G	Sensor	0.2523	0.0005	Columbia	Triaxial Mass Accelerometer	SA307TX	1644	50.56	0.00	6.68
Trans Bow Accel	G	Sensor	0.1265	0.0006							
Vert Stern Accel	G	Sensor	0.2509	-0.0096	Columbia	Triaxial Mass Accelerometer	SA307TX	1544	-48.88	0.00	5.80
Trans Stern Accel	G	Sensor	0.1262	-0.0012							
Electronics Batt	Volts	Sensor	3.3000	0.0000	NSWCCD	Voltage Divider	NA	NA	NA	NA	NA
Heading	Deg	Calculated	***	***	KVH	Fluxgate Compass	C-100	NA	44.19	0.00	7.08
Tracker Sensor	***	***	***	***	ArcSec				41.13	0.00	18.77

NOTE : Longitudinal Location - Positive Inches Fwd of Sta 10, Transverse Location - Positive Inches Starboard of Centerline, Vertical Location - Positive Inches Above Keel, NA - Not Applicable.

Table 7. Wave Height Sonics Located on MASK Bridge.

Gage Name	Units	Cal Factor (units /V)	Units Offset @ 0 V	Type Instrument	Mfg.	Model No.	Serial No.	Barcode No.	Location x (mm)	Location y (mm)
Bridge Wave Ht #1	mm	-76.60	+386	Ultrasonic Distance Transducer	Senix Corp	Ultra-SR-BP	00105878	039325	See Figure 7 & 8.	
Bridge Wave Ht #3	mm	-76.42	+394	Ultrasonic Distance Transducer	Senix Corp	Ultra-SR-BP	00105301	039326		
Bridge Wave Ht #4	mm	-76.50	+362	Ultrasonic Distance Transducer	Senix Corp	Ultra-SR-BP	00105678	039327		
Bridge Wave Ht #5	mm	-81.64	+387	Ultrasonic Distance Transducer	Senix Corp	Ultra-SR-BP	00105875	039328		
Bridge Wave Ht #6	mm	-76.78	+345	Ultrasonic Distance Transducer	Senix Corp	Ultra-SR-BP	00105740	039329		
Bridge Wave Ht #8	mm	-76.46	+395	Ultrasonic Distance Transducer	Senix Corp	Ultra-SR-BP	00105300	039330		



Table 8. Desired Wave Conditions as Defined by Test Matrix and Model Geometry.

### Full Scale Test Conditions

Ship Length : 466.00 ft

Wave/Hull Length	Wave Length (ft)	Wave Length (m)	Wave Period (sec)	Wave Freq (Hz)
0.75	349.50	6.71	8.26	0.1210
1.00	466.00	8.95	9.54	0.1048
1.25	582.50	11.18	10.67	0.0938
1.50	699.00	13.42	11.68	0.0856

### Model Scale Conditions - $\lambda = 46.6$

Ship Length : 10.00 ft

Wave/Hull Length	Wave Length (ft)	Wave Length (m)	Wave Period (sec)	Wave Freq (Hz)
0.75	7.50	2.29	1.210	0.826
1.00	10.00	3.05	1.398	0.716
1.25	12.50	3.81	1.563	0.640
1.50	15.00	4.57	1.712	0.584

Wave Heights				
Wave H/L	Wave Length / Hull Length			
	0.75	1.00	1.25	1.50
1/20	11.4 cm	15.2 cm	19.1 cm	22.9 cm
1/15	15.2 cm	20.3 cm	25.4 cm	30.5 cm
1/10	22.9 cm	30.5 cm	38.1 cm	45.7 cm
Wave H/L	Wave Length / Hull Length			
	0.75	1.00	1.25	1.50
1/20	4.50 in	6.00 in	7.50 in	9.00 in
1/15	6.00 in	8.00 in	10.00 in	12.00 in
1/10	9.00 in	12.00 in	15.00 in	18.00 in

Wave Steepness Coefficient - $(H)/(g \cdot T^2)$				
Wave H/L	Wave Length / Hull Length			
	0.75	1.00	1.25	1.50
1/20	0.008	0.008	0.008	0.008
1/15	0.011	0.011	0.011	0.011
1/10	0.016	0.016	0.016	0.016

Depth Effects Coefficient - $(d)/(g \cdot T^2)$				
Wave H/L	Wave Length / Hull Length			
	0.75	1.00	1.25	1.50
1/20	0.424	0.318	0.255	0.212
1/15	0.424	0.318	0.255	0.212
1/10	0.424	0.318	0.255	0.212

Table 9. Uncertainty Estimates for Instrumentation.

Parameter	Units	Type A Uncertainty *				Type B		Total	Total (% Max)
		Min	Max	N	Std Dev	U95	U95		
Acceleration, bow transverse	g	-1	+1	321	0.00668	0.0007	0.0081	0.0082	0.82
Acceleration, bow vertical	g	-1	+1	321	0.00379	0.0004	0.0010	0.0011	0.11
Acceleration, cg longitudinal	g	-1	+1	321	0.00049	0.0001	0.0020	0.0020	0.20
Acceleration, cg transverse	g	-1	+1	321	0.00649	0.0007	0.0033	0.0033	0.33
Acceleration, cg vertical	g	-1	+1	321	0.00236	0.0003	0.0108	0.0108	1.08
Acceleration, stern transverse	g	-1	+1	321	0.00694	0.0008	0.0098	0.0098	0.98
Acceleration, stern vertical	g	-1	+1	321	0.00337	0.0004	0.0209	0.0209	2.09
Angle, Pitch	deg	-50	+50	321	0.177	0.0198	0.64	0.64	1.28
Angle, Roll	deg	-90	+90	321	0.370	0.0413	0.77	0.77	2.67
Angle, Rudder	deg	-30	+30	321	0.029	0.0033	0.80	0.80	2.67
Heading	deg	0	360	321	0.733	0.0818	1.00	1.07	0.28
Model Speed	m/s	0.55	2.19	321	0.00836	0.0009	0.12	0.12	5.66
Propeller Shaft Speed	RPM	264	1093	321	4.28	0.48	1.78	1.84	0.17
Rudder Angular Rate, Max.	deg/s	-67.5	+67.2				1.61	1.61	2.40
Wave Height #1	mm	-381	+381				2.29	2.29	0.60
Wave Height #3	mm	-381	+381				3.42	3.42	0.90
Wave Height #4	mm	-381	+381				2.61	2.61	0.69
Wave Height #5	mm	-381	+381				3.22	3.22	0.85
Wave Height #6	mm	-381	+381				3.40	3.40	0.89
Wave Height #8	mm	-381	+381				1.89	1.89	0.50

\*Run DDG-51-0371

Table 10. Regular Wave Settings for Model 5514 Capsize Experiments.

Refined Wave Maker Settings From Testing						
$\lambda/L_{pp}$	$h/\lambda$	Freq (Hz)	Wave Height (in)	Long Bank RPM	Short Bank RPM	Stab. Lips
0.75	1/20	0.826	4.5	640	620	Up
	1/15		6.0	800	800	Up
	1/10		9.0	1250	1300	Up
1.00	1/20	0.716	6.0	690	670	Up
	1/15		8.0	900	860	Up
	1/10		12.0	1370	1410	Up
1.25	1/20	0.640	7.5	930	900	Up
	1/15		10.0	1100	1090	Up
	1/10		15.0	1550	1510	Up
1.50	1/20	0.584	9.0	1000	980	Up
	1/15		12.0	1210	1180	Up
	1/10		18.0	1600	1550	Up

Table 11. Summary of Roll Decay Roll Periods and Autopilot Coefficients,

EOSL KG=8.55m Gm=0.91m

Froude Number	Autopilot C1D Heading Error	Autopilot C2D Yaw Rate	Model Measured	FREDYN Interpolated	Geometry Based Target Roll Period	Ballast Based Roll Period Estimate
0.0	***	***	16.53	15.93	15.41	16.72
0.1	10.0	1.3	16.37	16.10	***	***
0.2	3.7	1.3	16.33	16.43	***	***
0.3	1.7	1.3	17.30	17.00	***	***
0.4	1.0	1.3	18.30	17.55	***	***

EOSL KG=8.22m Gm=1.25m

Froude Number	Autopilot C1D Heading Error	Autopilot C2D Yaw Rate	Model Measured	FREDYN Interpolated	Geometry Based Target Roll Period	Ballast Based Roll Period Estimate
0.0	***	***	13.46	13.77	13.19	13.48
0.1	10.0	1.3	13.55	13.83	***	***
0.2	5.1	1.3	13.59	14.07	***	***
0.3	2.2	1.3	13.60	14.47	***	***
0.4	1.3	1.3	14.47	15.05	***	***

Table 12. Summary of Turning Diameter Maneuvers.

Run Number	Full Scale Speed (knots)	Rudder Angle (degrees)	Steady Heel Angle (deg)	Advance (meters)	Transfer (meters)	Tactical Diameter (meters)
149	15.3	9.0	2.47	903	615	1242
150	14.8	-10.9	-3.33	1083	707	1421
151	14.5	-18.5	-4.01	563	389	753
152	14.5	-18.3	-3.88	670	402	758
153	14.4	20.8	3.27	642	360	676
154	14.5	28.5	3.27	543	287	562
155	22.9	-30.8	-3.69	604	304	580
157	21.73	-10.6	-6.92	789	640	1242
158	23.52	11.9	7.11	669	541	1050
159	15.3	-19.0	-8.14	635	386	752
160	14.8	25.1	8.01	569	337	608
161	14.5	-29.6	-7.94	536	316	598
162	14.5	27.6	7.68	478	322	613

Table 13. Summary of Zig-Zag Maneuvers.

	(Fn=0.2) 14.5 Knot 10-10 Zig-Zag			(Fn=0.2) 14.5 Knot 20-20 Zig-Zag		(Fn=0.3) 21.8 Knot 20-20 Zig-Zag	
Overshoot	Run 0163	Run 0164	Run 0164	Run 0172	Run 0173	Run 0182	Run 0183
Avg. Rudder angle	9.2	9.2	9	20.6	20.2	20.4	20.4
Initial Speed Kt	14.7	14.5	17	16.2	16.2	23	18.2
Avg. Trigger Angle	6.93	9.2	12.6	26	27.9	28.5	28.4
Model Average Overshoot	4.4	3.5	4.5	7.96	7.35	9.3	9.9
Overall Model Average Overshoot	4.13			7.66		9.60	

Table 14. Run Matrix for Intact 100kt Wind Limiting KG = 8.55m, EOSL Load Condition.

$\lambda/L$	$\lambda/h$	$F_n$	$\chi$ (deg)							
			0	15	30	45	60	75	90	105
0.75	20	0.0								
		0.1								
		0.2								
		0.3								
	15	0.0								
		0.1								
		0.2								
		0.3								
	10	0.0								
		0.1								
		0.2				213, 213	222, 223			
		0.3			195, 196	214, 215	218, 230	235, 236		

$\lambda/L$	$\lambda/h$	$F_n$	$\chi$ (deg)							
			0	15	30	45	60	75	90	105
1.00	20	0.0								
		0.1								
		0.2								
		0.3								
	15	0.0								
		0.1								
		0.2								
		0.3				237, 238	241, 242			
	10	0.0								
		0.1								
		0.2				239, 240	243, 248			
		0.3								

$\lambda/L$	$\lambda/h$	$F_n$	$\chi$ (deg)							
			0	15	30	45	60	75	90	105
1.25	20	0.0								
		0.1								
		0.2								
		0.3				395, 397				
	15	0.0								
		0.1								
		0.2				399				
		0.3			313	318, 311	315			
	10	0.0								
		0.1								
		0.2				323	324	337	386	
		0.3				325, 326	338, 339	388		

$\lambda/L$	$\lambda/h$	$F_n$	$\chi$ (deg)							
			0	15	30	45	60	75	90	105
1.50	20	0.0								
		0.1								
		0.2								
		0.3				399				
	15	0.0								
		0.1								
		0.2				404				
		0.3			407	405	392			
	10	0.0								
		0.1								
		0.2								
		0.3								

Key:

118	Max Roll Angle < 49.4 deg (75% of GZ curve)
419, 441	Max Roll Angle > 49.4 deg: in danger of capsizing (capsizing, dangerous roll)
143, 470, 486	Capsizing condition (capsizing, dangerous roll, acceptable roll)



Table 15. Run Matrix for Righting Arm Limiting KG = 8.22m, EOSL Load Condition.

$\lambda/L$	$\lambda/h$	$F_n$	$\chi$ (deg)							
			0	15	30	45	60	75	90	105
0.75	20	0.0								
		0.1								
		0.2								
		0.3								
		0.4								
	15	0.0								
		0.1								
		0.2								
		0.3								
		0.4								
	10	0.0								
		0.1								
		0.2								
		0.3			579, 580	582	581			
		0.4		581, 582	583, 584, 571, 472, 573	559				

$\lambda/L$	$\lambda/h$	$F_n$	$\chi$ (deg)							
			0	15	30	45	60	75	90	105
1.00	20	0.0								
		0.1								
		0.2								
		0.3								
		0.4								
	15	0.0								
		0.1								
		0.2								
		0.3								
		0.4								
	10	0.0								
		0.1								
		0.2								
		0.3		585	583	555				
		0.4		586, 587	584	556, 574				

$\lambda/L$	$\lambda/h$	$F_n$	$\chi$ (deg)							
			0	15	30	45	60	75	90	105
1.25	20	0.0								
		0.1								
		0.2								
		0.3								
		0.4								
	15	0.0								
		0.1								
		0.2								
		0.3								
		0.4								
	10	0.0								
		0.1								
		0.2								
		0.3	598	592	588	561	559	564, 567		
		0.4	597, 598	593, 594	589, 590	562, 563, 575	560	568, 569, 570		

Key.

118	Max Roll Angle < 53.6 deg (75% of GZ curve)
191	Max Roll Angle > 53.6 deg: in danger of capsize
143, 470, 486	Capsize condition (capsize, dangerous roll, acceptable roll)

Table 16. Roll Angle Matrix for Intact 100kt Wind Limiting KG = 8.55m, EOSL Load Condition.

$\lambda/L$	$\lambda/h$	$F_n$	$\gamma$ (deg)							
			0	15	30	45	60	75	90	105
0.75	20	0.0								
		0.1								
		0.2								
		0.3								
		0.4								
	15	0.0								
		0.1								
		0.2								
		0.3								
		0.4								
	10	0.0								
		0.1								
		0.2				26.2, 25.8	11.6, 12.2			
		0.3			32.8, 30.8	37.6, 34.2	19.2, 21.0	17.2, 18.7		
		0.4			76.1, 43.2, 90, 68.0, 61.9, 90, 90	90, 90, 67.4, 59.8, 61.8	26.6, 27.0			

$\lambda/L$	$\lambda/h$	$F_n$	$\chi$ (deg)								
			0	15	30	45	60	75	90	105	
1.00	20	0.0									
		0.1									
		0.2									
		0.3									
		0.4									
	15	0.0									
		0.1									
		0.2									
		0.3				28.2, 31.9	21.0, 22.4				
		0.4				32.1, 31.9	32.0, 31.9				
	10	0.0	28.6							28.1	
		0.1			28.2		34.2, 35.7	35.2, 35.8			
		0.2			34.6, 32.8	30.4, 30.9	19.4, 11.3	20.1, 18.9			
		0.3		29.6, 29.9	32.8, 42.1	27.5, 25.9	26.4, 26.9	21.8, 25.4			
		0.4		90, 90, 90, 90	90, 90, 90, 90	37.2, 33.4	38.2, 31.1	25.9, 34.6			

$\lambda/L$	$\lambda/h$	Fn	$\gamma$ (deg)							
			0	15	30	45	60	75	90	105
1.25	20	0.0								
		0.1								
		0.2								
		0.3				54.4, 23.9				
		0.4								
	15	0.0	19.9							
		0.1								
		0.2				19.0				
		0.3			29.9	25.8, 27.5	26.8			
		0.4			42.1, 42.9	40.8, 43.2	33.3, 34.4			
	10	0.0	28.4						30.5	
		0.1		34.3		32.5	30.6	30.1	27.6	
		0.2		26.9	35.3	30.1	35.7	34.8		
		0.3		33.3	38.7, 40.7	58.3, 48.1	45.1, 35.8	39.8		
		0.4	64.5, 90, 90	90, 90, 90, 90	90, 90, 90, 90	74.4, 90, 90, 90	69.0, 67.4, 90, 90, 61.2, 54.8	42.6		

$\lambda/L$	$\lambda/h$	$F_n$	$\chi$ (deg)							
			0	15	30	45	60	75	90	105
1.50	20	0.0								
		0.1								
		0.2								
		0.3				29.3				
		0.4				37.5	37.0			
	15	0.0								
		0.1								
		0.2		14.9		32.0				
		0.3		21.8	30.0	35.2	41.4			
		0.4			37.2	43.2	43.5			
	10	0.0								
		0.1								
		0.2								
		0.3								
		0.4								

Key:

40.6	Max Roll Angle < 49.4 deg (75% of GZ curve)
90, 67.4	Max Roll Angle > 49.4 deg: in danger of capsize (capsize, dangerous roll)
90, 64.5, 45.0	Capsize condition (capsize, dangerous roll, acceptable roll)

Table 17. Roll Angle Matrix for Righting Arm Limiting KG = 8.22m, EOSL Load Condition.

$\lambda/L$	$\lambda/h$	$F_n$	$\gamma$ (deg)							
			0	15	30	45	60	75	90	105
0.75	20	0.0								
		0.1								
		0.2								
		0.3								
		0.4								
	15	0.0								
		0.1								
		0.2								
		0.3								
		0.4								
	10	0.0								
		0.1								
		0.2								
		0.3			32.5, 34.5	36.4	39.5			
		0.4			48.1, 45.4	45.7, 44.7, 44.2, 41.7, 45.7	45.7			

$\lambda/L$	$\lambda/h$	$F_n$	$\chi$ (deg)							
			0	15	30	45	60	75	90	105
1.00	20	0.0								
		0.1								
		0.2								
		0.3								
		0.4								
	15	0.0								
		0.1								
		0.2								
		0.3								
		0.4								
	10	0.0								
		0.1								
		0.2								
		0.3		23.6	36.5	45.8				
		0.4		43.3, 48.6	45.2	52.3, 46.8				

$\lambda/L$	$\lambda/h$	$F_n$	$\chi$ (deg)							
			0	15	30	45	60	75	90	105
1.25	20	0.0								
		0.1								
		0.2								
		0.3								
		0.4								
	15	0.0								
		0.1								
		0.2								
		0.3								
		0.4								
	10	0.0								
		0.1								
		0.2								
		0.3	11.5	24.2	32.5	43.6	47.4	42.2, 45.6		
		0.4	52.6, 39.3	44.6, 41.9	46.1, 42.6	44.3, 35.0, 43.9	46.32	41.8, 28.5, 43.3		

Key

36.6	Max Roll Angle < 53.6 deg (75% of GZ curve)
55.2	Max Roll Angle > 53.6 deg: in danger of capsizing
90.0, 54.3, 48.1	Capsizing condition (capsizing, dangerous roll, acceptable roll)

Table 18. Wave Matrix for Intact 100kt Wind Limiting KG = 8.55m, EOSL Load Condition.

$\lambda/L$	$\lambda/h$	$F_n$	$\chi$ (deg)							
			0	15	30	45	60	75	90	105
0.75	20	0.0								
		0.1								
		0.2								
		0.3								
		0.4								
	15	0.0								
		0.1								
		0.2								
		0.3								
		0.4								
	10	0.0								
		0.1								
		0.2				(0.748, 10.85), (0.750, 10.03)	(0.753, 9.945), (0.754, 9.662)			
		0.3			(0.755, 9.640), (0.758, 9.978)	(0.753, 10.87), (0.754, 9.968)	(0.752, 9.662), (0.750, 9.224)	(0.757, 9.524), (0.757, 9.597)		
		0.4			(0.763, 9.933), (0.758, 10.89), (0.757, 10.02), (0.753, 10.75), (0.750, 10.04), (0.760, 10.10), (0.750, 10.03)	(0.747, 9.687) , (0.752, 10.64), (0.754, 9.968), (0.750, 10.02), (0.773, 10.30)	(0.760, 9.825), (0.752, 10.00)			

$\lambda/L$	$\lambda/h$	$F_n$	$\chi$ (deg)							
			0	15	30	45	60	75	90	105
1.00	20	0.0								
		0.1								
		0.2								
		0.3								
		0.4								
	15	0.0								
		0.1								
		0.2								
		0.3				(0.995, 14.79), (1.000, 14.42)	(0.994, 14.64), (1.004, 14.94)			
		0.4				(0.998, 14.73), (1.000, 14.30)	(0.993, 14.76), (1.005, 14.85)			
	10	0.0	(1.000, 10.10)						(0.998, 9.940)	
		0.1			(1.001, 10.37)		(0.998, 10.10), (1.002, 10.05)	(1.002, 9.642), (1.002, 10.00)		
		0.2			(1.007, 10.15), (1.000, 11.17)	(0.998, 9.440), (0.998, 9.778)	(0.985, 9.805), (0.998, 9.768)	(1.002, 9.746), (1.008, 9.773)		
		0.3		(0.996, 10.53), (0.995, 10.72)	(1.012, 9.718), (1.003, 10.32)	(0.993, 9.690), (1.006, 9.583)	(0.995, 9.703), (1.013, 10.08)	(1.010, 10.16), (0.995, 9.768)		
		0.4		(0.988, 10.07), (0.983, 9.595), (0.988, 10.35), (0.980, 9.265)	(0.982, 10.48), (0.995, 10.33), (1.020, 8.91), (0.998, 10.58)	(0.996, 9.888), (1.006, 9.888)	(0.992, 10.11), 294	(0.998, 9.613), (1.010, 9.935)		

Key:	(1.244, 9.990)	Max Roll Angle < 49.4 deg (75% of GZ curve)
	(1.223, 9.683), (1.252, 9.736)	Max Roll Angle > 49.4 deg: in danger of capsizing (capsizing, dangerous roll)
	(1.255, 9.928), (1.252, 9.972), (1.248, 9.768)	Capsizing condition (capsizing, dangerous roll, acceptable roll)

Table 18(cont.). Wave Matrix for Intact 100kt Wind Limiting KG = 8.55m, EOSL Load Condition.

$\lambda/L$	$\lambda/h$	$F_n$	$\alpha$ (deg)						
			0	15	30	45	60	75	90
1.25	20	0.0							
		0.1							
		0.2							
		0.3				(1.250, 18.14), (1.253, 19.10)			
		0.4							
	15	0.0	(1.248, 15.06)						
		0.1							
		0.2				(1.2420, 14.99)			
		0.3			(1.244, 14.85), (1.248, 14.58), (1.256, 14.39)	(1.248, 14.58), (1.256, 14.39)	(1.245, 14.21)		
		0.4			(1.258, 14.46), (1.244, 14.71)	(1.256, 14.68), (1.240, 14.93)	(1.252, 15.37), (1.244, 15.10)		
	10	0.0	(1.248, 9.788)						(1.248, 9.745)
		0.1		(1.244, 9.990)		(1.244, 10.39)	(1.260, 9.721)	(1.244, 9.662)	(1.266, 9.720)
		0.2		(1.238, 10.06)	(1.254, 10.04)	(1.245, 10.04)	(1.248, 9.677)	(1.260, 9.768)	
		0.3		(1.258, 9.970)	(1.252, 10.39)	(1.2467, 10.04), (1.254, 9.412)	(1.240, 9.748), (1.252, 9.776)	(1.248, 9.770)	
		0.4	(1.243, 10.05), (1.238, 10.10), (1.222, 9.800)	(1.255, 9.928), (1.250, 10.15), (1.265, 9.520), (1.237, 9.175)	(1.260, 10.05), (1.238, 9.990), (1.215, 9.478), (1.240, 9.283)	(1.252, 9.972), (1.228, 9.480), (1.254, 9.926), (1.243, 9.723)	(1.252, 9.604), (1.248, 9.736), (1.238, 9.683), (1.223, 8.905), (1.260, 9.277), (1.230, 9.283)	(1.245, 9.693)	

$\lambda/L$	$\lambda/h$	$F_n$	$\alpha$ (deg)						
			0	15	30	45	60	75	90
1.50	20	0.0							
		0.1							
		0.2							
		0.3				(1.250, 18.23)			
		0.4				(1.253, 19.20)	(1.2504, 18.23)		
	15	0.0							
		0.1							
		0.2		(1.503, 15.69)		(1.504, 14.59)			
		0.3		(1.493, 15.86)	(1.506, 14.85)	(1.496, 14.582)	(1.506, 14.20)		
		0.4			(1.506, 15.51)	(1.493, 14.80)	(1.506, 14.87)		
	10	0.0							
		0.1							
		0.2							
		0.3							
		0.4							

Key:

(1.244, 9.990)	Max Roll Angle < 49.4 deg (75% of GZ curve)
(1.223, 9.683), (1.252, 9.736)	Max Roll Angle > 49.4 deg: in danger of capsize (capsize, dangerous roll)
(1.255, 9.928), (1.252, 9.972), (1.248, 9.768)	Capsize condition (capsize, dangerous roll, acceptable roll)



Table 19. Wave Matrix for Righting Arm Limiting KG = 8.22m, EOSL Load Condition.

$\lambda/L$	$\lambda/h$	$F_n$	$\chi$ (deg)							
			0	15	30	45	60	75	90	105
0.75	20	0.0								
		0.1								
		0.2								
		0.3								
		0.4								
	15	0.0								
		0.1								
		0.2								
		0.3								
		0.4								
	10	0.0								
		0.1								
		0.2								
		0.3			(0.745, 11.07), (0.755, 10.85)	(0.782, 9.810)	(0.750, 9.927)			
		0.4			(0.743, 10.79), (0.742, 10.61)	(0.748, 10.10), (0.752, 10.26), (0.750, 10.08), (0.757, 9.743), (0.763, 10.42)	(0.758, 10.02)			

$\lambda/L$	$\lambda/h$	$F_n$	$\chi$ (deg)							
			0	15	30	45	60	75	90	105
1.00	20	0.0								
		0.1								
		0.2								
		0.3								
		0.4								
	15	0.0								
		0.1								
		0.2								
		0.3								
		0.4								
	10	0.0								
		0.1								
		0.2								
		0.3		(1.006, 10.22)	(1.002, 10.34)	(1.002, 9.550)				
		0.4		(0.996, 10.30), (1.006, 10.50)	(0.995, 10.08)	(0.987, 9.563), (0.993, 9.509)				

$\lambda/L$	$\lambda/h$	$F_n$	$\chi$ (deg)							
			0	15	30	45	60	75	90	105
1.25	20	0.0								
		0.1								
		0.2								
		0.3								
		0.4								
	15	0.0								
		0.1								
		0.2								
		0.3								
		0.4								
	10	0.0								
		0.1								
		0.2								
		0.3	(1.240, 9.957)	(1.240, 10.322)	(1.248, 10.22)	(1.245, 9.723)	(1.245, 9.443)	(1.245, 9.843), (1.242, 10.02)		
		0.4	(1.242, 10.06), (1.265, 10.30)	(1.255, 10.37), (1.255, 10.36)	(1.248, 10.06), (1.250, 10.57)	(1.240, 9.890), (1.237, 9.843), (1.248, 9.953)	(1.232, 9.383)	(1.235, 9.812), (1.257, 10.29), (1.245, 9.630)		

Key:

(0.742, 10.43)	Max Roll Angle < 53.6 deg (75% of GZ curve)
(1.247, 10.04)	Max Roll Angle > 53.6 deg, in danger of capsize
(1.250, 10.15), (1.252, 9.972), (1.266, 9.277)	Capsize condition (capsize, dangerous roll, acceptable roll)

This page intentionally left blank.

Table 20. EOSL Condition, Intact 100kt Wind Limiting KG=8.55m Test Versus FREDYN Results.

$\lambda/L$	$\lambda/h$	$F_n$	$\chi$ (deg)							
			0	15	30	45	60	75	90	105
0.75	20	0.0								
		0.1								
		0.2								
		0.3								
		0.4								
	15	0.0								
		0.1								
		0.2								
		0.3								
		0.4								
	10	0.0								
		0.1								
		0.2				$C_f$	$C_f$			
		0.3			$C_f$	$C_f$	$C_f$	$C_f$		
		0.4			$C_f$	$C_f$	$C_f$			

$\lambda/L$	$\lambda/h$	$F_n$	$\chi$ (deg)							
			0	15	30	45	60	75	90	105
1.00	20	0.0								
		0.1								
		0.2								
		0.3								
		0.4								
	15	0.0								
		0.1								
		0.2								
		0.3				$C_f$	$C_f$			
		0.4				$C_f$	$C_f$			
	10	0.0	$C_f$	$C_f$	$C_f$	$C_f$	$C_f$	$C_f$	$C_f$	
		0.1			$C_f$		$C_f$	$C_f$		
		0.2			$C_f$	$C_f$	$C_f$	$C_f$		
		0.3		$C_f$	$C_f$	$C_f$	$C_f$	$C_f$		
		0.4		$C_f$	$C_f$	$C_f$	$C_f$	$C_f$		

$\lambda/L$	$\lambda/h$	$F_n$	$\chi$ (deg)							
			0	15	30	45	60	75	90	105
1.25	20	0.0								
		0.1								
		0.2								
		0.3				$C_f$				
		0.4								
	15	0.0	$C_f$							
		0.1								
		0.2				$C_f$				
		0.3			$C_f$	$C_f$	$C_f$			
		0.4			$C_f$	$C_f$	$C_f$			
	10	0.0	$C_f$	$C_f$	$C_f$	$C_f$	$C_f$	$C_f$	$C_f$	$C_f$
		0.1		$N_f$		$C_f$	$C_f$	$C_f$	$C_f$	
		0.2		$C_f$	$C_f$	$C_f$	$C_f$	$C_f$		
		0.3		$C_f$	$C_f$	$C_f$	$C_f$	$C_f$		
		0.4	$C_f$	$C_f$	$C_f$	$C_f$	$C_f$	$C_f$		

$\lambda/L$	$\lambda/h$	$F_n$	$\chi$ (deg)							
			0	15	30	45	60	75	90	105
1.50	20	0.0								
		0.1								
		0.2								
		0.3				$C_f$				
		0.4				$C_f$	$C_f$			
	15	0.0								
		0.1								
		0.2		$C_f$		$C_f$				
		0.3		$C_f$	$C_f$	$C_f$	$C_f$			
		0.4			$C_f$	$C_f$	$C_f$			

Key:  
Model Test  
Results

FREDYN  
Prediction

	Max Roll Angle < 49.4 deg (75% of GZ curve)
	Max Roll Angle > 49.4 deg. in danger of capsizing
	Consistent capsizing condition
$C_f$	FREDYN predicted capsizing.
$N_f$	FREDYN predicted no capsizing.
$T_f$	FREDYN prediction terminated

Table 21. EOSL Condition, Righting Arm Limiting KG=8.22m Test Versus FREDYN Results.

$\lambda/L$	$\lambda/h$	$F_n$	$\chi$ (deg)							
			0	15	30	45	60	75	90	105
0.75	20	0.0								
		0.1								
		0.2								
		0.3								
		0.4								
	15	0.0								
		0.1								
		0.2								
		0.3								
		0.4								
	10	0.0								
		0.1								
		0.2					$C_f$			
		0.3			$N_f$	$C_f$	$C_f$			
		0.4			$C_f$	$C_f$	$C_f$			

$\lambda/L$	$\lambda/h$	$F_n$	$\chi$ (deg)							
			0	15	30	45	60	75	90	105
1.00	20	0.0								
		0.1								
		0.2								
		0.3								
		0.4								
	15	0.0								
		0.1								
		0.2								
		0.3								
		0.4					$C_f$			
	10	0.0	$T_f$	$C_f$	$C_f$	$C_f$	$C_f$	$C_f$	$C_f$	
		0.1					$C_f$	$C_f$		
		0.2				$C_f$	$C_f$	$C_f$		
		0.3		$N_f$	$C_f$	$C_f$	$C_f$	$C_f$		
		0.4		$C_f$	$C_f$	$C_f$	$C_f$	$C_f$		

$\lambda/L$	$\lambda/h$	$F_n$	$\chi$ (deg)							
			0	15	30	45	60	75	90	105
1.25	20	0.0								
		0.1								
		0.2								
		0.3								
		0.4								
	15	0.0								
		0.1								
		0.2				$C_f$	$C_f$			
		0.3				$C_f$				
		0.4				$C_f$	$C_f$			
	10	0.0	$C_f$	$C_f$	$C_f$	$C_f$	$C_f$	$C_f$	$C_f$	$C_f$
		0.1				$C_f$	$C_f$	$C_f$	$C_f$	
		0.2		$C_f$	$C_f$	$C_f$	$C_f$	$C_f$		
		0.3	$N_f$	$C_f$	$C_f$	$C_f$	$C_f$	$C_f$		
		0.4	$C_f$	$C_f$	$C_f$	$C_f$	$C_f$	$C_f$		

Key:		Max Roll Angle < 53.6 deg (75% of GZ curve)
		Max Roll Angle > 53.6 deg; in danger of capsizing
		Consistent capsizing condition
FREDYN Results	$C_f$	FREDYN predicted capsizing.
	$N_f$	FREDYN predicted no capsizing
	$T_f$	FREDYN prediction terminated
FREDYN Prediction		

Table 22. Motions for Model 5514 in Storm Sea State 8 – Hurricane Camille, Fn=0.1.

Full Scale Speed (kts): 7.25			Froude Number: 0.1					
Full Scale Sig Wave Ht (m): 12.21			Full Scale Modal Period (s): Approx 13.5 secs					
MOTIONS			RELATIVE WAVE HEADING					
			0	45	90	135	180	270
Roll	(deg)	SSA	4.08	23.38	22.79	15.33	4.09	19.19
Pitch	(deg)	SSA	4.09	4.13	1.16	5.79	6.15	1.09
Yaw	(deg)	SSA	8.83	14.17	23.84	22.04	12.44	18.01
Vert CG Accel	(g)	SSA	0.04	0.11	0.19	0.15	0.12	0.17
Trans CG Accel	(g)	SSA	0.07	0.38	0.44	0.32	0.08	0.36
Long CG Accel	(g)	SSA	0.01	0.01	0.01	0.04	0.04	0.01
Vert Bow Accel	(g)	SSA	0.09	0.17	0.22	0.30	0.31	0.19
Trans Bow Accel	(g)	SSA	0.07	0.34	0.46	0.34	0.08	0.37
Vert Stern Accel	(g)	SSA	0.08	0.15	0.19	0.23	0.22	0.17
Trans Stern Accel	(g)	SSA	0.07	0.41	0.41	0.31	0.07	0.34
Roll Rate	(deg/sec)	SSA	1.74	10.63	10.91	7.48	0.29	8.70
Pitch Rate	(deg/sec)	SSA	1.69	1.98	0.72	3.41	0.54	0.74
Yaw Rate	(deg/sec)	SSA	0.50	1.53	0.78	1.43	0.07	0.58
Rudder	(deg)	STD DEV	20.58	18.54	18.68	19.27	21.25	17.78
Shaft Speed	(rpm)	MEAN	308.09	295.44	298.01	289.84	289.70	300.36
Run Time	(min)	TOTAL	7.69	20.02	11.79	23.49	10.27	12.09
* Accelerations in Water Reference Frame at Location								
Sig Wave Ht	(m-full scale)		10.84	13.23	13.14	12.17	11.58	12.29



Table 23. Motions for Model 5514 in Storm Sea State 8 – Hurricane Camille, Fn=0.2.

Full Scale Speed (kts): 14.50				Froude Number: 0.2				
Full Scale Sig Wave Ht (m): 11.64				Full Scale Modal Period (s): Approx 13.5 secs				
MOTIONS			RELATIVE WAVE HEADING					
			0	45	90	135	180	270
Roll	(deg)	SSA	5.40	18.97	16.57	12.63	3.95	18.85
Pitch	(deg)	SSA	3.14	4.58	1.17	6.08	5.28	1.13
Yaw	(deg)	SSA	7.13	11.51	22.06	26.97	7.00	22.73
Vert CG Accel	(g)	SSA	0.03	0.09	0.18	0.22	0.15	0.20
Trans CG Accel	(g)	SSA	0.09	0.31	0.34	0.29	0.07	0.41
Long CG Accel	(g)	SSA	0.00	0.01	0.01	0.05	0.05	0.01
Vert Bow Accel	(g)	SSA	0.05	0.13	0.21	0.44	0.40	0.22
Trans Bow Accel	(g)	SSA	0.08	0.26	0.36	0.33	0.07	0.41
Vert Stern Accel	(g)	SSA	0.04	0.12	0.19	0.32	0.25	0.20
Trans Stern Accel	(g)	SSA	0.11	0.35	0.31	0.29	0.07	0.40
Roll Rate	(deg/sec)	SSA	1.67	7.90	8.33	6.41	1.87	9.05
Pitch Rate	(deg/sec)	SSA	0.99	1.87	0.76	4.15	3.77	0.78
Yaw Rate	(deg/sec)	SSA	0.59	1.81	0.87	1.60	0.44	0.63
Rudder	(deg)	STD DEV	16.23	15.52	17.40	17.03	13.41	17.16
Shaft Speed	(rpm)	MEAN	552.00	525.97	515.16	511.60	532.48	522.56
Run Time	(min)	TOTAL	22.04	13.89	17.10	14.67	25.77	10.86
* Accelerations in Water Reference Frame at Location								
Sig Wave Ht	(m-full scale)		9.79	13.03	11.99	12.90	9.63	12.52

Table 24. Motions for Model 5514 in Storm Sea State 8 – Hurricane Camille,  $F_n=0.3$ .

Full Scale Speed (kts): 21.75			Froude Number: 0.3			
Full Scale Sig Wave Ht (m): 12.68			Full Scale Modal Period (s): Approx 13.5 secs			
MOTIONS			RELATIVE WAVE HEADING			
			<b>45</b>	<b>90</b>	<b>135</b>	<b>270</b>
Roll	(deg)	SSA	19.11	11.73	9.80	21.75
Pitch	(deg)	SSA	4.15	1.08	6.52	1.12
Yaw	(deg)	SSA	10.93	19.36	26.67	19.85
Vert CG Accel	(g)	SSA	0.07	0.17	0.30	0.19
Trans CG Accel	(g)	SSA	0.33	0.23	0.25	0.43
Long CG Accel	(g)	SSA	0.01	0.01	0.06	0.02
Vert Bow Accel	(g)	SSA	0.11	0.20	0.61	0.20
Trans Bow Accel	(g)	SSA	0.29	0.25	0.29	0.44
Vert Stern Accel	(g)	SSA	0.09	0.18	0.41	0.19
Trans Stern Accel	(g)	SSA	0.37	0.22	0.25	0.42
Roll Rate	(deg/sec)	SSA	6.55	5.54	5.08	10.25
Pitch Rate	(deg/sec)	SSA	1.42	0.71	4.94	0.71
Yaw Rate	(deg/sec)	SSA	1.79	0.86	1.43	0.68
Rudder	(deg)	STD DEV	10.33	14.09	13.98	14.51
Shaft Speed	(rpm)	MEAN	815.62	804.11	792.85	811.61
Run Time	(min)	TOTAL	20.99	11.65	20.39	12.47
* Accelerations in Water Reference Frame at Location						
Sig Wave Ht	(m-full scale)		13.43	11.73	13.32	12.25

## REFERENCES

- [1] "Guide to the Expression of Uncertainty in Measurement," 1995, International Organization for Standardization (ISO), Geneva, Switzerland.
- [2] Scheffe, H., 1973, "A Statistical Theory of Calibration," **The Annals of Statistics**, 1(1), pp. 1-37.
- [3] Carroll, R. J., Spiegelman, C. H., and Sacks, J., 1988, "A Quick and Easy Multiple-Use Calibration-Curve Procedure," **Technometrics**, 30(2), pp. 137-141.
- [4] Coleman, H. W., and Steele, W. G., 1999, **Experimentation and Uncertainty Analysis for Engineers**, Second Edition, New York, John Wiley & Sons.
- [5] Moose, R.E., 1986, "The National Geodetic Survey Gravity Network," U.S. Department of Commerce, NOAA Technical Report NOS 121 NGS 39.
- [6] Ross, S. M., 1987, **Introduction to Probability and Statistics for Engineers and Scientists**, New York, John Wiley and Sons.
- [7] Lewis, E.V., 1989, **Principles of Naval Architecture – Volume III**, Society of Naval Architects and Marine Engineers, pp. 79.

**NSWCCD-50-TR-2006/020**

**Distribution**

	<i><b>Copies</b></i>	<i><b>Copies</b></i>
PMS500 (Syring, J.D. Captain) 197/3W 1333 ISAAC HULL AVE SE WASHINGTON NAVY YARD DC 20376	2	<b>NSWC, CARDEROCK DIVISION INTERNAL DISTRIBUTION</b>
	Code	Name Copies
NAVAL SEA SYSTEMS COMMAND	2	3442 TIC 1
ATTN: SEA 05H		5010 w/o Enclosure
1333 ISAAC HULL AVE SE STOP 1500		502 1
WASHINGTON NAVY YARD DC 20376-5100		51 Davis 1
		52 Day 1
NAVSEA 05H (Cimino, D.)	1	53 Johnston 1
197/2W		53 Strano 1
1333 ISAAC HULL AVE SE		54 Swzerc 1
WASHINGTON NAVY YARD DC 20376-5145		55 Applebee 1
		55 Hayden 5
DEFENSE TECHNICAL INFORMATION CENTER	1	55 Bishop 1
8725 JOHN KINGMAN ROAD SUITE 0944		55 Laverty 1
FORT BELVOIR VA 22060-6218		55 Lang 1
		55 Carrico 1
		55 Dipper 3
		55 Silver 1
		55 Smith 1
		55 Turner 1
		56 Ammeen 1
		56 Park 1